Excitation spectra of quantum matter without quasiparticles. I. Sachdev-Ye-Kitaev models

Maria Tikhanovskaya ⬤, Haoyu Guo ⬤, Subir Sachdev ⬤, and Grigory Tarnopolsky ⬤
Department of Physics, Harvard University, Cambridge, Massachusetts 02138, USA

We study the low-frequency spectra of complex Sachdev-Ye-Kitaev models at general densities. The analysis applies also to SU(M) magnets with random exchange at large M. The spectral densities are computed by numerical analysis of the saddle-point equations on the real frequency ω axis at zero temperature T. The asymptotic low-ω behaviors are found to be in excellent agreement with the scaling dimensions of irrelevant operators which perturb the conformally invariant critical states. Of possible experimental interest is our computation of the universal spin spectral weight of the SU(M) magnets at low ω and T; this includes a contribution from the time reparametrization mode, which is the boundary graviton of the holographic dual. This analysis is extended to a random t-J model in the following paper [M. Tikhanovskaya *et al.*, following paper, Phys. Rev. B **103**, 075142 (2021)].

I. INTRODUCTION

There has been much recent interest in solvable models [1–3] in the Sachdev-Ye-Kitaev (SYK) class as descriptions of compressible quantum many-body systems without quasiparticle excitations. These are models with random and all-to-all interactions, and their low-energy limit has the structure of (0+1)-dimensional conformal field theory [4]. Instead of quasiparticles, there are infinite towers of primary operators [5–8], all but a few of which have irrational scaling dimensions, and these describe the long-time dynamics of all local observables. We will examine a number of models of bosons and/or fermions in this paper; the boson or fermion, $a = \mathfrak{b}, f$, has a zero-temperature ($T = 0$) spectral density as a function of frequency ω of the form (for the case with $q = 4$ particle terms in the Hamiltonian)

$$\rho_a(\omega) = \begin{cases} \frac{g_{a+}(\omega)}{\sqrt{\omega}}, & \omega > 0 \\ \frac{g_{a-}(-\omega)}{\sqrt{-\omega}}, & \omega < 0. \end{cases} \quad (1.1)$$

Here $g_{a\pm}(\omega \to 0) = $ const and the main purpose of the present article is to describe the small-ω expansions of $g_{a\pm}(\omega)$ for a number of models of physical interest. These expansions depend upon the scaling dimensions and operator product expansions of the irrelevant primary operators and are also constrained by Luttinger-like theorems [9–11] and an emergent time-reparametrization symmetry [6,7]. We will compare conformal theory predictions with accurate numerical solutions of the SYK equations carried out directly on the real ω axis at $T = 0$ (as in the original paper of Ref. [1]) and find excellent agreement.

A related analysis has been carried out by Maldacena and Stanford [6]. They examined the particle-hole symmetric Majorana SYK model using numerical solutions of the SYK equations in imaginary time. All of our numerical analysis will be carried out in real time, using real-frequency spec-

tral functions; we will show that this allows higher precision and enables us to identify various subleading and nonlinear corrections. We also examine fermionic and bosonic models without particle-hole symmetry; the scaling dimensions for the particle-hole asymmetric fermionic models were obtained in Ref. [11].

Our results will also apply to the random quantum magnets with SU(M) symmetry which were studied in Ref. [1] in the limit of large M. Such models are of interest to condensed matter physics because of their "Mottness": They have constraints associated with strong on-site interactions, in contrast to the infinite-range interactions of the SYK models. For these magnets, we compute the local dynamic spin susceptibility $\chi_L(\omega)$. This quantity is potentially of experimental interest as a description of a quantum critical point in a disordered magnetic system studied by neutron scattering [12–16]. The time-reparametrization mode is the leading irrelevant operator determining the frequency dependence of χ_L and we find

$$\text{Im}\chi_L(\omega) \sim \tanh\left(\frac{\omega}{2T}\right)\left[1 - \mathcal{C}\gamma\omega\tanh\left(\frac{\omega}{2T}\right) - \cdots\right], \quad (1.2)$$

where the specific heat per spin component is equal to γT and $\mathcal{C}$ is a dimensionless number which is specified in (5.12) and (5.13) for our models. The leading term in (1.2) has been obtained earlier [4]. We obtain here the term proportional to $\mathcal{C}$; this is the contribution of the time-reparametrization mode, i.e., the boundary graviton in the holographic dual. Notice that this term has a prefactor of ω without a corresponding factor of $1/T$, which indicates the violation of scaling induced by an irrelevant operator. We show a plot of Imχ_L in Fig. 1; it is curious that this resembles observations in Refs. [13,14], and it would be worthwhile to investigate this further, especially in systems with greater randomness. Similar spectra should also apply to anomalous density fluctuations in the model of Ref. [17], and density fluctuations have
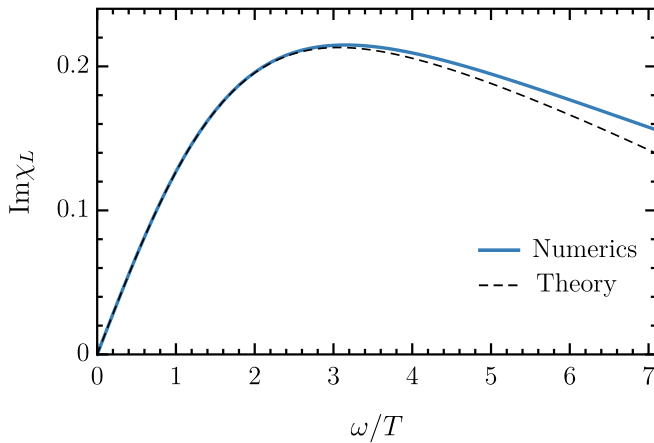
FIG. 1. Plot of the local dynamic spin susceptibility. The blue solid line is obtained from the numerical solution of the Schwinger-Dyson Eqs. (2.13) for $T/J = 0.1$. The black dashed line is the analytical result in (1.2) for $\mathcal{C}\gamma T \simeq 0.05$ with three higher-order terms in (1.3) included with their $T = 0$ expressions.

been investigated in momentum-resolved electron energy-loss spectroscopy [18,19] but for $\omega \gg T$.

In the limit of $T \to 0$, Eq. (1.2) predicts a discontinuous spectral density at zero frequency. We have computed higher-order terms at $T = 0$ for the particle-hole symmetric case [see Eq. (5.10)]

$$\text{Im}\chi_L(\omega) \sim \text{sgn}(\omega)\left[1 - \mathcal{C}\gamma|\omega| - \frac{7}{16}(\mathcal{C}\gamma)^2|\omega|^2 \right.$$
$$\left. - \mathcal{C}'|\omega|^{2.773\,54\ldots} + \frac{37}{48}(\mathcal{C}\gamma)^3|\omega|^3 - \cdots\right], \quad (1.3)$$

where the $|\omega|^2$ and $|\omega|^3$ terms are nonlinear corrections from the time-reparametrization mode and $\mathcal{C}'$ mode is a linear contribution of a second irrelevant operator with scaling dimension $h = 3.773\,54\ldots$. The $T > 0$ form of the $\mathcal{C}'$ term can be deduced from the imaginary part of (D24).

We have attempted to write this paper in a self-contained manner for condensed matter physicists. We will begin in Sec. II by defining the models of interest and recalling the leading conformally invariant results. A diagrammatic analysis of the conformal perturbation theory is presented in Sec. III, where we obtain the scaling dimensions of all primary operators and identify the operators associated with time reparametrization and an emergent U(1) gauge invariance. Section IV employs an alternative functional approach of Kitaev and Suh [7] which allows efficient treatment of particle-hole asymmetry, nonlinear corrections, and nonzero temperatures. Section V transforms our results from imaginary time to the spectral densities on the real-frequency axis. Section VI extends our analysis to models of bosonic random rotors, which have appeared in some recent studies of quantum phase transitions. Finally, our main numerical results are presented in Sec. VII, where we compare numerical solutions of the SYK equations on the real-frequency axis with the predictions of the conformal perturbation analysis.

The formalism developed in this paper for the SYK models will be applied to the *t-J* model in the following paper

[20]. We will dope the large-M SU(M) insulating quantum magnets described in the present paper by mobile charge carriers. The resulting theory of fractionalized particles, the spinons and holons, is described [21] by a set of Schwinger-Dyson equations similar to those presented in Sec. II. The following paper [20] presents the conformal corrections to a variety of gauge-invariant observables, including the electron spectral functions and the optical conductivity.

II. CONFORMAL SOLUTIONS FOR THE SYK MODELS

We begin by recalling the less-familiar models considered originally in Ref. [1], as these will connect directly to the *t-J* models considered in the following paper [20]. These are SU(M) spin models with the Hamiltonian

$$H_J = \sum_{\langle ij \rangle, \alpha\beta} J_{ij}\left(S_{i\alpha\beta}S_{j\beta\alpha} - \frac{1}{M}S_{i\alpha\alpha}S_{j\beta\beta}\right). \quad (2.1)$$

Here $\alpha = 1, \ldots, M$ is an SU(M) spin index, $S_{i\alpha\beta} = S_{i\beta\alpha}^\dagger$ is the spin operator on site i, and the $1/M$ term (which will be dropped in the large-M limit) is added to ensure it transforms in the adjoint of SU(M). Here we have chosen [4] to place the sites i on a high-dimensional lattice with coordination number z, and the J_{ij} are nearest-neighbor exchange interactions and Gaussian random variables with

$$\overline{J_{ij}} = 0, \quad \overline{J_{ij}^2} = \frac{J^2}{Mz}. \quad (2.2)$$

We will examine the model H_J in the limit of large z, followed by large M. Alternatively, we can consider the model on an N-site cluster, with all-to-all random exchange interactions; this was the model considered in Ref. [1], and the large-N limit leads to the same saddle-point equations as the large-z limit. However, the large-z limit allows us to consider transport properties of electrons in a lattice [4,22] using a *t-J* model, which we will described in the following paper.

The properties of the SU(M) spin models depend upon the representation of SU(M) realized by the states on each site i. The most common choices correspond to the formulations in terms of fermionic and bosonic *spinons*. The fermionic spinon case corresponds to the representation with a single column of boxes in the SU(M) Young tableaux, with the spin operator

$$S_{i\alpha\beta} = f_{i\alpha}^\dagger f_{i\beta} \quad (2.3)$$

expressed in terms of fermionic spinons $f_{i\alpha}$. This induces a U(1) gauge symmetry

$$f_{i\alpha}(\tau) \to f_{i\alpha}(\tau)e^{i\phi_i(\tau)}. \quad (2.4)$$

The physical Hilbert space must be U(1) gauge symmetric, which implies that the gauge charge is conserved, and we consider the representation

$$\sum_\alpha f_{i\alpha}^\dagger f_{i\alpha} = \kappa M, \qu(2.5)$$

with κM boxes in the Young tableaux. We will take the large-M limit at fixed κ.

Similarly, the bosonic spinon case corresponds to a different SU(M) representation with a Young tableaux of a single row of boxes, and the spin operator

$$S_{i\alpha\beta} = \mathfrak{b}_{i\alpha}^\dagger \mathfrak{b}_{i\beta}, \quad (2.6)$$

with the U(1) gauge charge constraint

$$\sum_\alpha \mathfrak{b}_{i\alpha}^\dagger \mathfrak{b}_{i\alpha} = \kappa M. \qquad (2.7)$$

The fermionic spinon representation defined by (2.3) and (2.5) and the bosonic spinon representation defined by (2.6) and (2.7) are the same only for $\kappa M = 1$.

Along with the SU(M) spin models recalled above, our results apply also to the complex SYK model (with a $q = 4$ fermion Hamiltonian)

$$H_{\text{SYK}} = \frac{1}{2N^{3/2}} \sum_{i,j,k,\ell=1}^N J_{ij;k\ell} f_i^\dagger f_j^\dagger f_k f_\ell - \mu_f \sum_i f_i^\dagger f_i, \quad (2.8)$$

where $J_{ij;k\ell}$ are independent random numbers with $\overline{|J_{ij;k\ell}|^2} = J^2$. The advantage of this model is that only a single large-N limit is required, and there is no analog of the subsequent large-M limit required for the models above. However, as we discussed in Sec. I, this simplicity comes at a cost: We lose the Mottness that is present in the spin (and t-J) models and is important for condensed matter applications. The analog of the fermion constraint in (2.5) is now

$$\langle f_i^\dagger f_i \rangle = \kappa, \qquad (2.9)$$

with no sum over i. Analogously to the fermionic SYK model, we can define the bosonic SYK model as

$$H_{\text{SYK}} = \frac{1}{2N^{3/2}} \sum_{i,j,k,\ell=1}^N J_{ij;k\ell} \mathfrak{b}_i^\dagger \mathfrak{b}_j^\dagger \mathfrak{b}_k \mathfrak{b}_\ell - \mu_\mathfrak{b} \sum_i \mathfrak{b}_i^\dagger \mathfrak{b}_i, \quad (2.10)$$

along with the constraint

$$\langle \mathfrak{b}_i^\dagger \mathfrak{b}_i \rangle = \kappa. \qquad (2.11)$$

We remark that the bosonic models defined above have a kinetic term $\mathfrak{b}^\dagger \partial_\tau \mathfrak{b}$ in the Lagrangian formalism.

All of the above models have a common set of saddle-point equations, which we now describe. We introduce a two-point Green's function in imaginary time τ at a finite temperature T:

$$\begin{aligned} G_f(\tau) &= -\langle T_\tau(f(\tau) f^\dagger(0)) \rangle, \\ G_b(\tau) &= -\langle T_\tau(\mathfrak{b}(\tau) \mathfrak{b}^\dagger(0)) \rangle. \end{aligned} \qquad (2.12)$$

In both cases the large-N Schwinger-Dyson (SD) equations look identical and read, for $\tau \in (0, \beta)$,

$$\begin{aligned} G_a(i\omega_n) &= \frac{1}{i\omega_n + \mu_a - \Sigma_a(i\omega_n)}, \\ \Sigma_a(\tau) &= J^2 G_a(\tau)^{q/2} G_a(\beta - \tau)^{q/2-1}, \end{aligned} \qquad (2.13)$$

where the index $a = f, \mathfrak{b}$ denotes fermions or bosons, $\beta = 1/T$ is the inverse temperature, μ_a is the chemical potential, and we assume that q is an even integer. The models described above have $q = 4$, but we will also present some results for general q. For the fermionic case the Matsubara frequency is $\omega_n = \frac{2\pi}{\beta}(n + \frac{1}{2})$ and for the bosonic case $\omega_n = \frac{2\pi}{\beta} n$. The two-point Green's function satisfies the Kubo-Martin-Schwinger condition $G_a(\tau) = \zeta_a G_a(\beta + \tau)$, where $\zeta_\mathfrak{b} = 1$ and $\zeta_f = -1$.

It is well known that Eqs. (2.13) admit a conformal solution in the IR region, where $1/J \ll \tau \ll \beta - 1/J$,

$$G_a^c(\tau) = -b_a^\Delta \left(\frac{\beta J}{\pi} \sin \frac{\pi \tau}{\beta} \right)^{-2\Delta} e^{2\pi \mathcal{E}_a(1/2 - \tau/\beta)},$$

$$\Sigma_a^c(\tau) = -J^2 b_a^{1-\Delta} \left(\frac{\beta J}{\pi} \sin \frac{\pi \tau}{\beta} \right)^{-2(1-\Delta)} e^{2\pi \mathcal{E}_a(1/2 - \tau/\beta)},$$

$$(2.14)$$

where $\Delta = 1/q$, $\mathcal{E}_a$ is the asymmetry parameter which implicitly depends on μ, and the dimensionless constant prefactor b_a is

$$\begin{aligned} b_f &= \frac{(1 - 2\Delta) \sin 2\pi \Delta}{4\pi \cos \pi (\Delta + i\mathcal{E}_f) \cos \pi (\Delta - i\mathcal{E}_f)}, \\ b_\mathfrak{b} &= \frac{(1 - 2\Delta) \sin 2\pi \Delta}{4\pi \sin \pi (\Delta + i\mathcal{E}_\mathfrak{b}) \sin \pi (\Delta - i\mathcal{E}_\mathfrak{b})}. \end{aligned} \qquad (2.15)$$

When we work in frequency space, it turns out to be convenient to use the asymmetry angles θ_a related to $\mathcal{E}_a$ by

$$\begin{aligned} e^{2\pi \mathcal{E}_a} &= \zeta_a \frac{\sin(\theta_a + \pi \Delta)}{\sin(\theta_a - \pi \Delta)}, \\ e^{-2i\theta_f} &= \frac{\cos \pi (\Delta + i\mathcal{E}_f)}{\cos \pi (\Delta - i\mathcal{E}_f)}, \\ e^{-2i\theta_\mathfrak{b}} &= -\frac{\sin \pi (\Delta + i\mathcal{E}_\mathfrak{b})}{\sin \pi (\Delta - i\mathcal{E}_\mathfrak{b})}. \end{aligned} \qquad (2.16)$$

Therefore, we can find

$$b_a = \zeta_a \frac{1 - 2\Delta}{\pi} \frac{\sin(\theta_a + \pi \Delta) \sin(\theta_a - \pi \Delta)}{\sin 2\pi \Delta}. \qquad (2.17)$$

Notice that $\mathcal{E}_\mathfrak{b} = 0$ for $\theta_\mathfrak{b} = \pi/2$ and $\mathcal{E}_f = 0$ for $\theta_f = 0$. Also, $\pi \Delta < \theta_\mathfrak{b} < \pi/2$ and $-\pi \Delta < \theta_f < \pi \Delta$.

Below we will study the structure of the conformal corrections to the large-z and large-M saddle point of H_J in (2.1) and the large-N saddle point of H_{SYK} in (2.8). The Schwinger-Dyson equations at the saddle point are identical in the two models, so the conformal corrections will also be the same. However, once we go beyond the saddle point and examine four-point correlators, there will be differences between the two models. We will not address these differences here.

III. CONFORMAL PERTURBATIONS

In this section we describe a useful view point on the SYK models as a conformal field theory (CFT) perturbed by infinite set of irrelevant operators. Although this approach is not rigorous and has caveats, which we mention below, it clarifies understanding of some results and can correctly predict $1/\beta J$ and $1/(\beta J)^2$ corrections to the free energy (see Appendix A). We will turn to a more complete approach to similar results in Sec. IV.

For simplicity, in this section we consider only the fermionic SYK model (2.8) with zero chemical potential $\mu = 0$, as the generalization to $\mu \neq 0$ is described in Sec. IV. It was shown in Refs. [23–25] that this model has an infinite set of bilinear primary operators $O_h^A(\tau)$ and $O_h^S(\tau)$, which can be schematically represented as $O_{h_n}^A = f_i^\dagger \partial_\tau^{2n+1} f_i$ and $O_{h_n}^S = f_i^\dagger \partial_\tau^{2n} f_i$ for $n = 0, 1, 2, \dots$. To compute the scaling
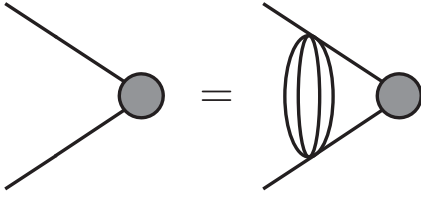
FIG. 2. Diagrammatic representation of the Dyson-Schwinger Eqs. (3.2), after dropping the bare terms. The internal loop has $q - 2$ powers of G^c (this diagram is for $q = 6$).

dimensions of the operators $O_h^{A/S}(\tau)$ we consider three-point functions

$$v_h^{A/S}(\tau_1, \tau_2, \tau_0) = \langle f(\tau_1) f^\dagger(\tau_2) O_h^{A/S}(\tau_0) \rangle. \quad (3.1)$$

Then we can derive the Dyson-Schwinger equations for the three-point functions in the IR region and we can drop the bare terms to obtain [23]

$$v_h^{A/S}(\tau_1, \tau_2, \tau_0) = \int d\tau_3 d\tau_4 K_{A/S}(\tau_1, \tau_2; \tau_3, \tau_4) v_h^{A/S}$$
$$\times (\tau_3, \tau_4, \tau_0), \quad (3.2)$$

where the kernels $K_{A/S}$ are

$$K_{A/S}(\tau_1, \tau_2; \tau_3, \tau_4)$$
$$= -\left[\frac{q}{2} \pm \left(\frac{q}{2} - 1 \right) \right] J^2 G^c(\tau_{13}) G^c(\tau_{24}) G^c(\tau_{34})^{q-2}. \quad (3.3)$$

Diagrammatically, Eqs. (3.2) are represented in Fig. 2.

Emergent conformal symmetry in the IR region fixes the functional form of the three-point functions up to the structure constants c_h^A and c_h^S,

$$v_h^A(\tau_1, \tau_2, \tau_0) = \frac{c_h^A b^\Delta \operatorname{sgn}(\tau_{12})}{|J\tau_{12}|^{2\Delta - h} |J\tau_{10}|^h |J\tau_{20}|^h},$$
$$v_h^S(\tau_1, \tau_2, \tau_0) = \frac{c_h^S b^\Delta \operatorname{sgn}(\tau_{10}) \operatorname{sgn}(\tau_{20})}{|J\tau_{12}|^{2\Delta - h} |J\tau_{10}|^h |J\tau_{20}|^h}. \quad (3.4)$$

It can be shown that for arbitrary h the three-point functions $v_h^{A/S}$ satisfy the equation [6,7,24,25]

$$\int d\tau_3 d\tau_4 K_{A/S}(\tau_1, \tau_2; \tau_3, \tau_4) v_h^{A/S}(\tau_3, \tau_4, \tau_0)$$
$$= k_{A/S}(h) v_h^{A/S}(\tau_1, \tau_2, \tau_0), \quad (3.5)$$

where $k_{A/S}(h)$ are given by the formulas

$$k_A(h) = \frac{\Gamma(2\Delta - h)\Gamma(2\Delta + h - 1)}{\Gamma(2\Delta - 2)\Gamma(2\Delta + 1)} \left(1 - \frac{\sin \pi h}{\sin 2\pi \Delta} \right),$$
$$k_S(h) = \frac{\Gamma(2\Delta - h)\Gamma(2\Delta + h - 1)}{\Gamma(2\Delta - 1)\Gamma(2\Delta)} \left(1 + \frac{\sin \pi h}{\sin 2\pi \Delta} \right). \quad (3.6)$$

These formulas can be verified by taking the limit $|\tau_0| \to \infty$ in (3.5) and then evaluating the integrals over $\tau_{3,4}$. Therefore, comparing (3.5) with (3.2), we have to set

$$k_A(h) = 1, \quad k_S(h) = 1, \quad (3.7)$$

which define the anomalous scaling dimensions of the operators $O_h^{A/S}(\tau)$.

The SYK model can be viewed as some conformal field theory perturbed by this infinite set of irrelevant primary operators. In the case of zero chemical potential $\mu = 0$ there is an exact particle-hole symmetry and thus only O_h^A operators can appear in the action. This situation exactly coincides with the case of the Majorana SYK model, where instead of complex fermions f_i we have Majorana fermions χ_i. Therefore, in what follows we omit letter A for brevity and write for the effective action of the Majorana SYK model

$$S_{SYK} = S_{CFT} + \sum_h g_h \int_0^\beta d\tau \, O_h(\tau), \quad (3.8)$$

where O_h has anomalous dimensions $h = h_0, h_1, h_2, h_3, \dots$ and $h_0 = 2, h_1 \simeq 3.77, h_2 \simeq 5.68$, etc., which are found from the equation $k_A(h) = 1$. (Note that we will often use the subscript i to represent the subscript h_i, e.g., $g_{h_2} \equiv g_2$).

The expression for the full two-point function reads

$$G(\tau_{12}) = -\frac{1}{Z} \int D\chi \frac{1}{N} \chi_i(\tau_1) \chi_i(\tau_2) e^{-S_{SYK}}. \quad (3.9)$$

Therefore, using conformal perturbation theory, we find

$$G(\tau_{12}) = G^c(\tau_{12}) + \sum_h g_h \int d\tau_3 \frac{1}{N} \langle \chi_i(\tau_1) \chi_i(\tau_2) O_h(\tau_3) \rangle$$
$$- \frac{1}{2} \sum_{h,h'} g_h g_{h'} \int d\tau_3 d\tau_4 \frac{1}{N} \langle \chi_i(\tau_1) \chi_i(\tau_2)$$
$$\times O_h(\tau_3) O_{h'}(\tau_4) \rangle + \cdots, \quad (3.10)$$

where we used that $G^c(\tau_{12}) = -\frac{1}{N} \langle \chi_i(\tau_1) \chi_i(\tau_2) \rangle$ and averaging of the correlation functions is implicitly performed with the action S_{CFT} and involves only connected diagrams. The higher correlation functions are fixed by conformal invariance up to the structure constants c_h and $c_{h_1 h_2 h_3}$,

$$\frac{1}{N} \langle \chi_i(\tau_1) \chi_i(\tau_2) O_h(\tau_3) \rangle = \frac{c_h b^\Delta \operatorname{sgn}(\tau_{12})}{|J\tau_{12}|^{2\Delta - h} |J\tau_{13}|^h |J\tau_{23}|^h},$$
$$\frac{1}{N} \langle \chi_i(\tau_1) \chi_i(\tau_2) O_{h_1}(\tau_3) O_{h_2}(\tau_4) \rangle$$
$$= \sum_h \frac{c_h c_{h h_1 h_2} b^\Delta \operatorname{sgn}(\tau_{12}) |\tau_{14}|^{h_{12}}}{|J\tau_{12}|^{2\Delta} |J\tau_{34}|^{h_1 + h_2} |\tau_{13}|^{h_{12}}} x^h \, {}_2F_1(h, h + h_{12}, 2h, x), \quad (3.11)$$

where $h_{12} = h_1 - h_2$ and $x = \frac{\tau_{12}\tau_{34}}{\tau_{13}\tau_{24}}$. Alternatively, they can be found from the operator product expansion (OPE)

$$\frac{1}{N} \chi_i(\tau_1) \chi_i^\dagger(\tau_2) = \frac{b^\Delta \operatorname{sgn}(\tau_{12})}{|J\tau_{12}|^{2\Delta}} + \frac{1}{N} \sum_h \frac{c_h b^\Delta \operatorname{sgn}(\tau_{12})}{|J\tau_{12}|^{2\Delta - h}}$$
$$\times \mathcal{C}_h(\tau_{12}, \partial_2) O_h(\tau_2),$$
$$O_{h_1}(\tau_1) O_{h_2}(\tau_2) = \frac{N\delta_{hh'}}{|J\tau_{12}|^{2h}} + \sum_{h''} c_{h_1 h_2 h_3} |J\tau_{12}|^{h_3 - h_1 - h_2}$$
$$\times \mathcal{C}_{123}(\tau_{12}, \partial_2) O_{h_3}(\tau_2), \quad (3.12)$$

where $b = \frac{1}{2\pi}(1 - 2\Delta) \tan \pi \Delta$ and the operators $\mathcal{C}_h$ and $\mathcal{C}_{123}$ generate all descendants and are determined by the functional form of the three-point functions. The structure constants c_h

are [6]

$$c_h^2 = \frac{1}{(q-1)b^\Delta} \frac{h-1/2}{\pi \tan(\pi h/2)} \frac{\Gamma(h)^2}{\Gamma(2h)} \frac{1}{k'_{\rm A}(h)} \quad (3.13)$$

and $c_{hh'h''}$ have a much more complicated form and were computed in Refs. [8,26]. The OPE formulas (3.12) should not include the $h_0 = 2$ operator, since it was shown in [6] that this operator breaks conformal symmetry in the SYK model. Moreover, we note that c_h is divergent for $h_0 = 2$. Nevertheless, let us assume that we deal with unbroken CFT and can include the operator O_{h_0} in the OPE formulas assuming the limit $h_0 \to 2$.[1]

For the first-order correction to the two-point function at zero temperature $\beta = \infty$ we find

$$\delta G_h(\tau_{12}) = g_h \int_{-\infty}^{+\infty} d\tau_3 \frac{c_h b^\Delta \mathrm{sgn}(\tau_{12})}{|J\tau_{12}|^{2\Delta-h}|J\tau_{13}|^h|J\tau_{23}|^h}$$
$$= -G^c(\tau_{12}) \frac{\alpha_h}{|J\tau_{12}|^{h-1}}, \quad (3.14)$$

where α_h and g_h are related as

$$g_h^2 = J^2(q-1)b^\Delta k'_{\rm A}(h) \frac{h-1/2}{\pi \tan(\pi h/2)} \frac{\Gamma(h)^2}{\Gamma(2h)} \alpha_h^2. \quad (3.15)$$

We note that g_0 has to be divergent for $h_0 = 2$ in order for α_0 to be finite. Also, we remark that all $g_h \propto J$ are dimensionful couplings, whereas α_h are dimensionless constants. The analysis in Sec. IV establishes that α_0 is indeed finite, and we will confirm this in our numerical results.

For the second-order correction we find, using (3.11),

$$\delta^2 G_{hh'}(\tau_{12}) = -\frac{1}{2} g_h g_{h'} \int d\tau_3 d\tau_4 \frac{1}{N} \langle \chi_i(\tau_1) \chi_i(\tau_2) O_h(\tau_3)$$
$$\times O_{h'}(\tau_4) \rangle$$
$$= -G^c(\tau_{12}) \frac{a_{hh'} \alpha_h \alpha_{h'}}{2|J\tau_{12}|^{h+h'-2}}, \quad (3.16)$$

where the coefficients $a_{hh'}$ are functions of h, h', and Δ and we will find some of them explicitly in Sec. IV using resonance theory.

It is instructive to use these conformal perturbation methods to also compute the free energy. We describe this in Appendix A; one term is at variance with another discussion [28].

IV. KITAEV-SUH RESONANCE THEORY

In this section we review the renormalization and resonance formalism developed in [7,11,22] and extend it to nonlinear order. The theory provides a framework for understanding the corrections due to physics at higher-energy scales in SYK-type models.

---

[1]Perhaps this approach can be justified if the SYK model is considered as a limit of some conformal SYK model for which $h_0 = 2 - \epsilon_0$ and $\epsilon_0 \to 0$ (see [27] and Appendix H in [6]).

To linear order, the corrected Green's function in (3.10), $G(\tau) = -\langle \mathcal{T}_\tau f(\tau) f^\dagger(0) \rangle$, can be written as

$$G(\tau) = G^c(\tau) \left(1 - \sum_h \frac{\alpha_h}{(\beta J)^{h-1}} \mathcal{F}_h(\tau/\beta) + \cdots \right). \quad (4.1)$$

Here recall that $G^c(\tau)$ is the conformal Green's function, β is the inverse temperature, and J denotes some UV energy scale, which is usually taken to be the SYK coupling. In addition, $\mathcal{F}_h$ is some universal scaling functions that will be computed later in (4.55). The sum runs over a set of discrete numbers $\{h_i\}$ that will be determined in Sec. IV A. Although the resonance formalism is a direct consequence of Schwinger-Dyson equations, the structure of the corrections is consistent with the CFT interpretation of the SYK-type model. The numbers $\{h_i\}$ can be interpreted as the scaling dimensions of primary operators $\{O_h\}$ in the SYK CFT that appears in the OPE of $f(\tau) f^\dagger(0)$. The dimensionless coefficients α_h parametrize the deformation away from the SYK CFT, as in (3.8). The exact values of α_h require solving the full Schwinger-Dyson equations in the UV and they are usually extracted from numerics.

In SYK-type models, the operators $O_0^{\rm S}$ (there may be several) of scaling dimension $h_0^{\rm S} = 1$ and $O_0^{\rm A}$ of scaling dimension $h_0^{\rm A} = 2$ are special: They are the conserved charges of U(1) and time-reparametrization symmetry, respectively. These symmetries are emergent and spontaneously broken in the IR, but also explicitly broken by the deformation δS which exists in the UV. Therefore, δS provides the effective action for the these pseudo-Nambu-Goldstone modes. For the time-reparametrization symmetry, this is the well-known Schwarzian action.

The resonance formalism was first developed in [7] for the Majorana SYK model, where the Green's function is always antisymmetric in time and $\mathcal{F}_h$ is obtained for generic temperature. In [11] the formalism was extended to the complex SYK model which has a U(1) symmetry, and $\mathcal{F}_h$ is obtained at zero temperature for generic U(1) charge. In [22] the theory was further extended to the t-J model, a coupled system of both fermions and bosons, and the scaling function $\mathcal{F}_h$ was obtained for generic temperature and U(1) charge. In all these previous works, the correction is only calculated for linear order in α_h, which only provides information about the spectral weight $\rho_a(\omega)$ around $\omega = 0$. In this paper we extend the formalism to arbitrary nonlinear order in α_h, which shows excellent agreement with large-q expansion and numerics at finite q; it can now extrapolate the spectral weight $\rho_a(\omega)$ up to finite ω/J.

A. Linear order correction

We summarize previous works on linear order resonance theory [7,11,22]. Our discussion will be based on the SD equation, abstractly written as

$$G = G_*[\Sigma], \quad \Sigma = \Sigma_*[G] + \sigma. \quad (4.2)$$

Here G and Σ are regarded as bilocal fields and G_* and Σ_* are functionals that define the saddle point. In addition, σ is a bilocal field referred to as the UV source. The conformal solution (G^c, Σ^c) is exact if $\sigma = 0$. In the bosonic and fermionic SYK$_q$ models, $G_*[\Sigma](\tau_1, \tau_2) = -(1/\Sigma)(\tau_1, \tau_2)$

(in the sense of functional inverse), $\Sigma_*[G](\tau_1, \tau_2) = (-)^{\epsilon_a} J^2 G(\tau_1, \tau_2)^{q/2} [-G(\tau_2, \tau_1)]^{q/2-1}$, and $\sigma(\tau_1, \tau_2) = (\partial_{\tau_1} - \mu)\delta(\tau_1 - \tau_2)$. Here σ is referred to as the UV source because it contains high-frequency Fourier components. We also note that the self-energy Σ is shifted from the usual definition by σ.

If we are interested in the IR physics $J^{-1} \ll |\tau| \lesssim \beta$, the UV source σ can be treated as a small perturbation, the small parameter being the ratio between IR and UV scales $1/(\beta J)^{h-1}$ or $1/|J\tau|^{h-1}$. To calculate the linear response, we expand the SD Eqs. (4.2) around the conformal saddle point (G^c, Σ^c) to linear order

$$G = G^c + \delta G, \quad \Sigma = \Sigma^c + \delta\Sigma \tag{4.3}$$

and obtain

$$\delta G = W_\Sigma \delta\Sigma, \quad \delta\Sigma = W_G \delta G + \sigma, \tag{4.4}$$

where we defined W_Σ and W_G as

$$W_\Sigma = \left.\frac{\delta G_*}{\delta\Sigma}\right|_{\Sigma^c}, \quad W_G = \left.\frac{\delta\Sigma_*}{\delta G}\right|_{G^c}. \tag{4.5}$$

Finally, a simple analysis yields [11]

$$\delta G = (1 - \underbrace{W_\Sigma W_G}_{K_G})^{-1} W_\Sigma \sigma, \quad \delta\Sigma = (1 - \underbrace{W_G W_\Sigma}_{K_\Sigma})^{-1}\sigma. \tag{4.6}$$

Here we defined two kernels $K_G = W_\Sigma W_G$ and $K_\Sigma = W_G W_\Sigma$. We remark that K_G is exactly the one-rung diagrams that one needs to sum to compute the four-point functions [6,7]. By construction, the nonzero spectra of K_G and K_Σ are the same.

In what follows we adopt a convenient notation used in Ref. [11] for writing functions which have discontinuity at $\tau = 0$ and different behavior for negative and positive τ. Namely, we write all functions as two component vectors, where the first component is for $\tau > 0$ and the second one is for $\tau < 0$. We refer to this as a plus/minus basis. For example, the conformal solution for the Green's function $G_a^c(\tau)$ and self-energy $\Sigma_a^c(\tau)$ at zero temperature can be written as

$$G_a^c(\tau) = -\begin{pmatrix} e^{\pi\mathcal{E}_a}, & \tau > 0 \\ \zeta_a e^{-\pi\mathcal{E}_a}, & \tau < 0 \end{pmatrix} \frac{b_a^\Delta}{|J\tau|^{2\Delta}},$$

$$\Sigma_a^c(\tau) = -\begin{pmatrix} e^{\pi\mathcal{E}_a}, & \tau > 0 \\ \zeta_a e^{-\pi\mathcal{E}_a}, & \tau < 0 \end{pmatrix} \frac{J^2 b_a^{1-\Delta}}{|J\tau|^{2(1-\Delta)}}, \tag{4.7}$$

where the constant b_a is given in (2.17), $\zeta_\flat = 1$, and $\zeta_f = -1$. In what follows we suppress the index $a = f, \flat$ in various functions for brevity and only keep ζ factors where they are needed.

To proceed with the analysis, we note that the conformal saddle point possesses SL(2, R) symmetry and therefore we can break up (4.6) into irreducible representations of SL(2, R) labeled by h, and a convenient basis for this purpose at zero temperature is

$$\delta G(\tau) = \delta\vec{G}|J\tau|^{1-h}G^c(\tau),$$

$$\delta\Sigma(\tau) = \delta\vec{\Sigma}|J\tau|^{1-h}\Sigma^c(\tau),$$

$$\sigma(\tau) = \sum_h \vec{\sigma}_h |J\tau|^{1-h}\Sigma^c(\tau)u(\tau), \tag{4.8}$$

where $\delta\vec{G} = (\delta G_+, \delta G_-)^{\mathrm{T}}$, $\delta\vec{\Sigma} = (\delta\Sigma_+, \delta\Sigma_-)^{\mathrm{T}}$, and $\vec{\sigma}_h = (\sigma_{h+}, \sigma_{h-})^{\mathrm{T}}$ are all two-component columns according to our new notation and the source $\sigma(\tau)$ is written in the IR region with the window function $u(\tau)$ and positive real numbers h (for details about this representation of the source σ see Ref. [7]). In this basis, W_Σ and W_G, and K_G and K_Σ become (2×2)-dimensional matrices. So for the fermionic and bosonic SYK$_q$ models (2.13), we can find

$$\delta\Sigma_*(\tau)|_{G^c} = \left[\frac{q}{2}\frac{\delta G(\tau)}{G^c(\tau)} + \left(\frac{q}{2} - 1\right)\frac{\delta G(-\tau)}{G^c(-\tau)}\right]\Sigma^c(\tau), \tag{4.9}$$

and using the basis (4.8) we write it as

$$\delta\Sigma_*(\tau)|_{G^c} = W_G \delta\vec{G}|J\tau|^{1-h}\Sigma^c(\tau), \tag{4.10}$$

where W_G becomes a 2×2 matrix given by the formula

$$W_G = \begin{pmatrix} q/2 & q/2 - 1 \\ q/2 - 1 & q/2 \end{pmatrix}. \tag{4.11}$$

To find expression for the operator W_Σ we use the Fourier transform written in our convenient plus/minus basis

$$\int\begin{pmatrix} a_+|\tau|^{-\alpha}, & \tau > 0 \\ a_-|\tau|^{-\alpha}, & \tau < 0 \end{pmatrix}e^{i\omega\tau}d\tau = \begin{pmatrix} a'_+|\omega|^{\alpha-1}, & \omega > 0 \\ a'_-|\omega|^{\alpha-1}, & \omega < 0 \end{pmatrix},$$

$$\begin{pmatrix} a'_+ \\ a'_- \end{pmatrix} = M(\alpha)\begin{pmatrix} a_+ \\ a_- \end{pmatrix}, \tag{4.12}$$

where the 2×2 matrix $M(\alpha)$ has the form

$$M(\alpha) = \Gamma(1 - \alpha)\begin{pmatrix} i^{1-\alpha} & i^{\alpha-1} \\ i^{\alpha-1} & i^{1-\alpha} \end{pmatrix},$$

$$M(\alpha)^{-1} = \frac{\Gamma(\alpha)}{2\pi}\begin{pmatrix} i^{-\alpha} & i^\alpha \\ i^\alpha & i^{-\alpha} \end{pmatrix}. \tag{4.13}$$

In the Fourier space the basis (4.8) takes the form

$$\delta G(i\omega) = F(h)\delta\vec{G}|\omega/J|^{h-1}G^c(i\omega),$$

$$\delta\Sigma(i\omega) = \Phi(h)\delta\vec{\Sigma}|\omega/J|^{h-1}\Sigma^c(i\omega), \tag{4.14}$$

where the matrices $F(h)$ and $\Phi(h)$ are

$$F(h) = -i\sqrt{\frac{\Gamma(2\Delta)}{\Gamma(2 - 2\Delta)}}b^{1/2}\begin{pmatrix} e^{i\theta} & 0 \\ 0 & -e^{-i\theta} \end{pmatrix}M(2\Delta - 1 + h)$$

$$\times\begin{pmatrix} e^{\pi\mathcal{E}} & 0 \\ 0 & \zeta e^{-\pi\mathcal{E}} \end{pmatrix},$$

$$\Phi(h) = -i\sqrt{\frac{\Gamma(2 - 2\Delta)}{\Gamma(2\Delta)}}b^{1/2}\begin{pmatrix} e^{-i\theta} & 0 \\ 0 & -e^{i\theta} \end{pmatrix}M(1 - 2\Delta + h)$$

$$\times\begin{pmatrix} e^{\pi\mathcal{E}} & 0 \\ 0 & \zeta e^{-\pi\mathcal{E}} \end{pmatrix} \tag{4.15}$$

and we used formulas for $G^c(i\omega)$ and $\Sigma^c(i\omega)$ in the Fourier space at zero temperature

$$G^c(i\omega) = -\frac{iC}{J}\begin{pmatrix} e^{-i\theta} \\ -e^{i\theta} \end{pmatrix}|\omega/J|^{2\Delta-1},$$

$$\Sigma^c(i\omega) = -\frac{iJ}{C}\begin{pmatrix} e^{i\theta} \\ -e^{-i\theta} \end{pmatrix}|\omega/J|^{1-2\Delta}, \tag{4.16}$$

where we defined $C \equiv \sqrt{\Gamma(2 - 2\Delta)/\Gamma(2\Delta)}b^{\Delta - 1/2}$. Notice that there are no ζ factors in (4.16). The operator W_Σ connects linear corrections $\delta\Sigma$ and δG as $\delta G = W_\Sigma \delta\Sigma$ and has a simple form in the Fourier space

$$\delta G_*(i\omega)|_{\Sigma^c} = G^c(i\omega)^2 \delta\Sigma(i\omega). \qquad (4.17)$$

Thus, using (4.14) and $G^c(i\omega)\Sigma^c(i\omega) = -1$, we find

$$F(h)\delta\vec{G} = -\Phi(h)\delta\vec{\Sigma} \qquad (4.18)$$

and therefore W_Σ acts on $\delta\vec{\Sigma}$ as a matrix $W_\Sigma(h) = -F(h)^{-1}\Phi(h)$ and is given by the formula [11]

$$W_\Sigma(h) = \frac{\Gamma(2\Delta - 1 + h)\Gamma(2\Delta - h)}{\Gamma(2\Delta)\Gamma(2\Delta - 1)\sin(2\pi\Delta)} \begin{pmatrix} \sin(\pi h + 2\theta) & -\sin(2\pi\Delta) + \sin(2\theta) \\ -\sin(2\pi\Delta) - \sin(2\theta) & \sin(\pi h - 2\theta) \end{pmatrix}. \qquad (4.19)$$

We note that the matrix $W_\Sigma(h)$ has the same form for bosonic and fermionic SYK models and the only difference is the range of asymmetry angle θ in these two cases. The matrix $K_G(h)$ is a product of two matrices $W_\Sigma(h)$ and W_G, so $K_G(h) = W_\Sigma(h)W_G$. Therefore, (4.6) reads

$$\delta G = \frac{1}{1 - K_G(h)}W_\Sigma(h)\sigma. \qquad (4.20)$$

For generic h, $1 - K_G(h)$ is nonsingular and therefore the response δG is negligible at IR scales. We need to recall that a physical source σ is supported only in the UV and we expect that a nonsingular response δG is also constrained in the UV region. To get an IR response, $1 - K_G(h)$ should be singular, so the possible h that appears in (4.1) is selected by the condition

$$\det[1 - K_G(h)] = 0. \qquad (4.21)$$

For the particle-hole symmetric case $\mu = 0$, this equation is equivalent to $k_{A/S}(h) = 1$, where $k_{A/S}(h)$ are defined in (3.6).

For the resonant values of $h = h_*$, the apparent singularity in (4.20) is regulated by the window function $u(\tau)$ which restricts σ to be supported only on UV scales. Following [7,11], we obtain

$$\delta G(\tau) = \sum_{h=h_*} \frac{1}{K_G'(h)}W_\Sigma(h)\vec{\sigma}_h|J\tau|^{1-h}G^c(\tau), \qquad (4.22)$$

where the sum goes over all resonances h_* which are the solutions of (4.21). The derivative of matrix $K_G'(h)$ is

$$\frac{1}{K_G'(h)} = \frac{v_h w_h}{k_G'(h)}, \qquad (4.23)$$

where v_h and w_h are the corresponding right and left eigenvectors of $K_G(h)$, respectively, which have the eigenvalue $k_G(h) = 1$ and are normalized as $w_h v_h = 1$. Finally, we can rewrite (4.22) in the form

$$\delta G(\tau) = -\sum_{h=h_*} \alpha_h v_h \frac{G^c(\tau)}{|J\tau|^{h-1}},$$
$$\alpha_h = -\frac{w_h W_\Sigma(h)\vec{\sigma}_h}{k_G'(h)}. \qquad (4.24)$$

We remark that the values of $\vec{\sigma}_h$ and thus α_h are not accessible in the IR because a physical UV source such as $\sigma(\tau) = (\partial_\tau - \mu)\delta(\tau)$ is highly singular and the task of decomposing it into asymptotic power laws perhaps is equivalent to solving the full Schwinger-Dyson equations. Below in Sec. VII we present numerical results for α_h of the first few resonances in the bosonic and fermionic SYK$_4$ models. The UV parameters α_h depend on the asymmetry angle θ and q.[2] Below we present explicit formulas for the eigenvalues and eigenvectors of the matrix $K_G(h)$,

$$k_{A/S}(h, \theta) = \frac{\Gamma(2\Delta - h)\Gamma(2\Delta + h - 1)}{\Gamma(2\Delta + 1)\Gamma(2\Delta - 1)}\left(2\Delta - 1 + \frac{\cos 2\theta \sin \pi h}{\sin 2\pi\Delta} \mp \sqrt{P}\right),$$

$$v_h^{A/S}(\theta) = \frac{1}{1 + (2\Delta - 1)\frac{\sin \pi h}{\sin 2\pi\Delta}}\begin{pmatrix} \frac{\sin 2\theta}{\sin 2\pi\Delta}(2\Delta - 1 - \cos \pi h) \pm \sqrt{P} \\ 1 + \frac{\sin 2\theta}{\sin 2\pi\Delta} + (2\Delta - 1)\frac{\sin(\pi h - 2\theta)}{\sin 2\pi\Delta} \end{pmatrix}, \qquad (4.25)$$

where

$$P = \sin(2\theta)^2\left(1 - \frac{\sin(\pi h)^2}{\sin(2\pi\Delta)^2}\right) + \left(\cos(2\theta) + (2\Delta - 1)\frac{\sin \pi h}{\sin 2\pi\Delta}\right)^2. \qquad (4.26)$$

Also $w_h^{A/S}(\theta)$ can be expressed through $v_h^{S/A}(\theta)$ as $w_h^{A/S}(\theta) = v_h^{S/A}(-\theta)^T\sigma_z/[v_h^{S/A}(-\theta)^T\sigma_z v_h^{A/S}(\theta)]$, where σ_z is the third

Pauli matrix and one can check that $w_h^{A/S}v_h^{S/A} = 0$. We note that for $\theta = 0$ the eigenvalues $k_{A/S}(h)$ in (4.25) coincide with the definition (3.6). Though for the nonzero asymmetry angle θ there is no symmetry under $\tau \to -\tau$, we still label eigenvalues and eigenvectors with A/S indices. We denote by $h^{A/S}$ solutions of the equations $k_{A/S}(h, \theta) = 1$ and numerate them as $h_0^{A/S}, h_1^{A/S}, h_2^{A/S}, \ldots$. For these solutions we denote α_h by $\alpha_0^{A/S}, \alpha_1^{A/S}, \ldots$ and similarly $v_0^{A/S}, v_1^{A/S}, \ldots$. In Fig. 3 we plot

---

[2]We note that α_0 for the $h_0 = 2$ resonance in the Majorana SYK model was computed numerically in Ref. [6] and denoted there by α_G. Moreover, α_G was defined with respect to $\mathcal{J} = 2^{(1-q)/2}\sqrt{q}J$ and therefore for $q = 4$ we have $\alpha_0 = \sqrt{2}\alpha_G$.
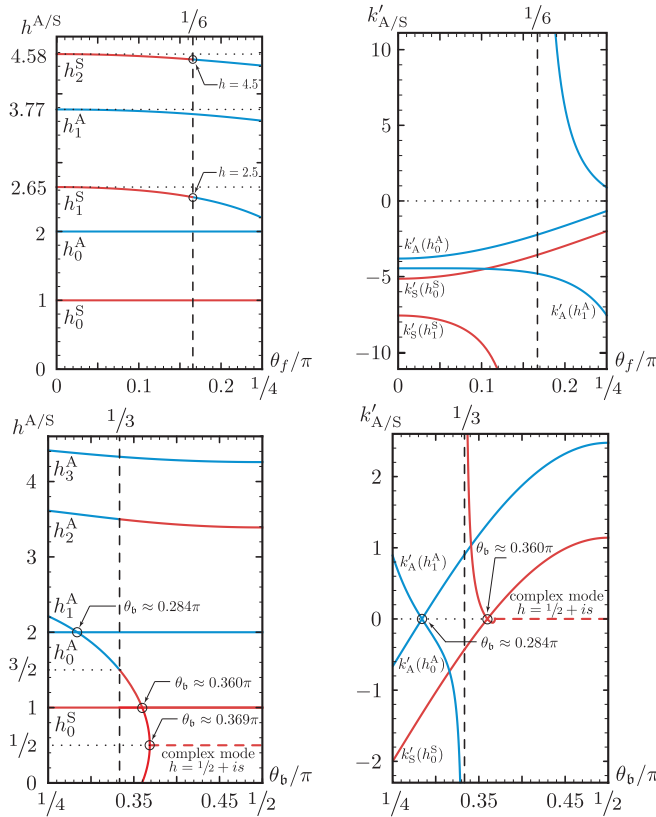
FIG. 3. Plots of the resonance values $h^{A/S}$ and corresponding $k'_{A/S}(h^{A/S})$ for the fermionic and bosonic $q = 4$ SYK models as functions of the asymmetry angles θ_f and $\theta_\flat$. Here $h^{A/S}$ are solutions of the equations $k_{A/S}(h, \theta) = 1$, where $k_{A/S}$ are defined in (4.25). The red and blue lines are solutions of the equations $k_S(h) = 1$ and $k_A(h) = 1$, respectively.

$h^{A/S}$ and the corresponding $k'_{A/S}(h^{A/S})$ for the fermionic and bosonic SYK_4 models as functions of the asymmetry angles θ_f and $\theta_\flat$. We remark that in the fermionic model for $\theta_f = \pi/6$ some solutions of the equation $k_S(h) = 1$ (red lines) go into solutions of $k_A(h) = 1$ (blue lines); nevertheless, we still denote the dimension of the whole line by h^A. In the bosonic case this happens for $\theta_\flat = \pi/3$. The resonances $h_0^A = 2$ and $h_0^S = 1$ are related to reparametrization and U(1) symmetries, respectively, and do not depend on the asymmetry angle θ_f or $\theta_\flat$. According to Eq. (4.24), the mode $h_0^S = 1$ gives a constant correction to the Green's function and represents a response of the asymmetry parameter $\mathcal{E}$ (or θ) to a change of the chemical potential μ. Therefore, in the conformal two-point function (4.7) this mode is already taken into account. Moreover, it was shown in [11] that the $h_0^S = 1$ resonance leads to the Luttinger relations

$$Q \equiv \frac{1}{2} - \frac{1}{NM} \sum_{i\alpha} \langle f_{i\alpha}^\dagger f_{i\alpha} \rangle = \frac{\theta_f}{\pi} + \left(\frac{1}{2} - \Delta \right) \frac{\sin 2\theta_f}{\sin 2\pi \Delta},$$

$$S \equiv \frac{1}{NM} \sum_{i\alpha} \langle \flat_{i\alpha}^\dagger \flat_{i\alpha} \rangle = \frac{\theta_\flat}{\pi} + \left(\frac{1}{2} - \Delta \right) \frac{\sin 2\theta_\flat}{\sin 2\pi \Delta} - \frac{1}{2}. \tag{4.27}$$

We note an interesting behavior of the operator h_1^A in the bosonic SYK model. For $\theta_\flat > 0.284\pi$ [exact value $\theta_{\flat 1} = \frac{1}{2} \cos^{-1}(\frac{-2}{3\pi})$] the resonance h_1^A is less than the $h_0^A = 2$ mode and becomes the leading contribution to the Green's function. At $\theta_\flat = \pi/3$ we have $h_1^A = 3/2$ and for $\theta_\flat = 0.360\pi$ [exact value $\theta_{\flat 2} = \frac{1}{2} \cos^{-1}(\frac{-2}{\pi})$] we find that $h_1^A = 1$ and therefore we should expect violation of the Luttinger relations (4.27). We indeed confirm this numerically below in Sec. VII. For $\theta_\flat > 0.360\pi$ the resonance h_1^A becomes less than one and therefore gives a divergent contribution to the Green's function for large τ. In terms of the discussion of Sec. III, this means that the operator $O_{h_1^A}$ becomes relevant and thus it violates the basis of the analysis of Secs. III and IV. Interestingly, for $\theta_\flat > 0.360\pi$ we see that another operator of dimension $1 - h_1^A$ appears and both operators merge at $\theta_\flat = 0.369\pi$ [exact value $\theta_{\flat 3} = \frac{1}{2} \cos^{-1}(\frac{1}{2} - \frac{3}{8\pi})$] and $h = 1/2$ and go to the complex plane. This is a well-known scenario, discussed in [29–31]. In the context of the SYK-like models it was also found in [32].

We chose normalization of $v_h^{A/S}$ in (4.25) such that at $\theta = 0$ it is $v_h^{A/S} = (\pm 1, 1)^T$ and $w_h^{A/S} = \frac{1}{2}(\pm 1, 1)$ for arbitrary h and thus the value of α_0 for $h_0^A = 2$ mode is in agreement with the previous works [6,7].

We remark that for the fermionic SYK model at zero chemical potential $\mu = 0$ ($\theta_f = 0$) we have

$$\alpha_h^S = \frac{\sigma_{h+}^S - \sigma_{h-}^S}{k'_S(h)} = 0, \tag{4.28}$$

where we used that the source $\sigma(\tau)$ has to be antisymmetric under $\tau \to -\tau$ due to the particle-hole symmetry. Thus, in this case only h^A operators contribute to the two-point function.

B. Nonlinear order corrections

In this section we present the generalization of the above resonance formalism to linear in α_h order. In the CFT interpretation, we are computing corrections to Green's functions due to double insertion of irrelevant operators, for example, $\iint d\tau_3 d\tau_4 \langle f(\tau_1) f^\dagger(\tau_2) O_h(\tau_3) O_{h'}(\tau_4) \rangle$, which is expected to be proportional to $1/|\tau_{12}|^{2\Delta + h + h' - 2}$. In terms of the Schwinger-Dyson equation, this corresponds to double insertion of the UV source σ. We will develop a recursive procedure that enables computation of correction up to arbitrary order.

For simplicity, we will restrict the procedure to zero temperature and comment on finite temperature later. Our strategy is to treat (4.2) as a perturbation problem and expand G and Σ to nth order in σ:

$$\begin{aligned} G &= G^c + \delta G + \delta^2 G + \cdots + \delta^n G, \\ \Sigma &= \Sigma^c + \delta \Sigma + \delta^2 \Sigma + \cdots + \delta^n \Sigma. \end{aligned} \tag{4.29}$$

Expanding (4.2) accordingly and matching order by order, we have

$$\delta^k G = \delta^k G_*[\Sigma], \quad \delta^k \Sigma = \delta^k \Sigma_*[G], \quad k \geq 2. \tag{4.30}$$

We can calculate $\delta^k G$ and $\delta^k \Sigma$ order by order recursively. To do so we rewrite the above equations as

$$\delta^k G = W_\Sigma \delta^k \Sigma + \bar\delta^k G_*[\Sigma], \quad \delta^k \Sigma = W_G \delta^k G + \bar\delta^k \Sigma_*[G], \tag{4.31}$$

where we have explicitly separated out the pieces depending on $\delta^k G$ and $\delta^k \Sigma$, which are all linear. The rest are written as $\bar\delta^k G_*$ and $\bar\delta^k \Sigma_*$ and they depend nonlinearly on the corrections of order 1 through $k-1$. We can readily write down the solution for $\delta^k G$ and $\delta^k \Sigma$:

$$\delta^k G = \frac{1}{1 - W_\Sigma W_G}(W_\Sigma \bar\delta^k \Sigma_*[G] + \bar\delta^k G_*[\Sigma]), \tag{4.32}$$

$$\delta^k \Sigma = \frac{1}{1 - W_G W_\Sigma}(W_G \bar\delta^k G_*[\Sigma] + \bar\delta^k \Sigma_*[G]). \tag{4.33}$$

The starting point of the recursion is the δG and $\delta \Sigma$ computed from linear resonance theory. Because all $\delta^k G$ and $\delta^k \Sigma$ are power laws in both the time and frequency domains, the expansion of $\bar\delta^k G_*$ and $\bar\delta^k \Sigma_*$ and the action of W_Σ and W_G can be carried out analytically and automated on a computer. At finite temperature, the recursion is harder to implement because $\delta^k G$ and $\delta^k \Sigma$ are usually hypergeometric functions whose complexity increases with k.

As an example, we find the second-order correction for the bosonic and fermionic SYK$_q$ models. The Schwinger-Dyson Eqs. (4.2) take the forms

$$G_*[\Sigma](i\omega) = \frac{-1}{\Sigma(i\omega)}, \tag{4.34}$$

$$\Sigma_*[G](\tau) = (-)^{\epsilon_a} J^2 G(\tau)^{q/2} G(-\tau)^{q/2-1}. $$

In Sec. IV A we derived the linear order response for the resonance h,

$$\delta_h G(\tau) = -\alpha_h v_h \frac{G^c(\tau)}{|J\tau|^{h-1}}, \tag{4.35}$$

where $v_h = (v_{h+}, v_{h-})$ is the right eigenvector of the matrix $K_G(h) = W_\Sigma(h)W_G$ with the eigenvalue $k_G(h) = 1$, so $K_G(h)v_h = v_h$. Using (4.34), we can calculate

$$\bar\delta^2 G_* = -\sum_{h,h'} \frac{\delta_h \Sigma(i\omega)\delta_{h'}\Sigma(i\omega)}{\Sigma^c(i\omega)^3} = \sum_{h,h'} \frac{\delta_h G(i\omega)\delta_{h'}G(i\omega)}{G^c(i\omega)}, \tag{4.36}$$

where we used that $G^c(i\omega)\Sigma^c(i\omega) = -1$ and $\delta_h G(i\omega) = G^c(i\omega)^2 \delta_h \Sigma(i\omega)$ and the sum over h and h' goes over all resonances. Using (4.14), we find, for the linear order response in the Fourier space,

$$\delta_h G(i\omega) = -\alpha_h F(h)v_h |\omega/J|^{h-1} G^c(i\omega), \tag{4.37}$$

where the matrix $F(h)$ is given in (4.15) and acts on the vector v_h. Therefore, we find

$$\frac{\delta_h G(i\omega)\delta_{h'}G(i\omega)}{G^c(i\omega)} = \alpha_h \alpha_{h'}[F(h)v_h F(h')v_{h'}]|\omega/J|^{h+h'-2}G^c(i\omega), \tag{4.38}$$

where we introduced the special notation $v_h v_{h'} \equiv (v_{h+}v_{h'+}, v_{h-}v_{h'-})$. Finally, we return to the coordinate space and obtain, for the second variation of $\bar\delta^2 G_*$,

$$\frac{\bar\delta^2 G_*(\tau)}{G^c(\tau)} = \sum_{h,h'} F(h+h'-1)^{-1}[F(h)v_h F(h')v_{h'}]\frac{\alpha_h \alpha_{h'}}{|J\tau|^{h+h'-2}}. \tag{4.39}$$

The second variation of $\Sigma_*[G_c]$ reads

$$\frac{\bar\delta^2 \Sigma_*(\tau)}{\Sigma^c(\tau)} = \frac{q-2}{8}\left(q\frac{\delta_h G(\tau)\delta_{h'}G(\tau)}{G^c(\tau)G^c(\tau)} + (q-4)\frac{\delta_h G(-\tau)\delta_{h'}G(-\tau)}{G^c(-\tau)G^c(-\tau)} + q\frac{\delta_h G(\tau)\delta_{h'}G(-\tau)}{G^c(\tau)G^c(-\tau)} + q\frac{\delta_h G(-\tau)\delta_{h'}G(\tau)}{G^c(-\tau)G^c(\tau)}\right). \tag{4.40}$$

Using our vector notation for $v_h = (v_{h+}, v_{h-})$ and $\bar v_h = (v_{h-}, v_{h+})$, we obtain

$$\frac{\bar\delta^2 \Sigma_*(\tau)}{\Sigma^c(\tau)} = \sum_{h,h'} \frac{1}{8}(q-2)[q(v_h + \bar v_h)(v_{h'} + \bar v_{h'}) - 4\bar v_h \bar v_{h'}]\frac{\alpha_h \alpha_{h'}}{|J\tau|^{h+h'-2}}. \tag{4.41}$$

Therefore, the full second correction to $G(\tau)$ reads

$$\frac{\delta^2 G(\tau)}{G^c(\tau)} = -\frac{a_{hh'}\alpha_h \alpha_{h'}}{|J\tau|^{h+h'-2}}, \tag{4.42}$$

where the two-component vector $a_{hh'}$ is given by the formula

$$a_{hh'} = -[1 - W_\Sigma(h+h'-1)W_G]^{-1}\{F(h+h'-1)^{-1}[F(h)v_h F(h')v_{h'}]$$
$$+ \frac{1}{8}(q-2)W_\Sigma(h+h'-1)[q(v_h + \bar v_h)(v_{h'} + \bar v_{h'}) - 4\bar v_h \bar v_{h'}]\}. \tag{4.43}$$

The general formula for the two-point function can be written as

$$G(\tau) = G^c(\tau)\left(1 - \sum_h \frac{\alpha_h v_h}{|J\tau|^{h-1}} - \sum_{h,h'}\frac{a_{hh'}\alpha_h \alpha_{h'}}{|J\tau|^{h+h'-2}} - \sum_{h,h',h''}\frac{a_{hh'h''}\alpha_h \alpha_{h'}\alpha_{h''}}{|J\tau|^{h+h'+h''-3}} - \cdots\right), \tag{4.44}$$

where v_h, $a_{hh'}$, $a_{hh'h''}$, etc., are two-component vectors. For example, for the $h_0^A = 2$ mode and the $q = 4$ case we find

$$v_0^A = \begin{pmatrix} 1 - \frac{3}{2}\sin 2\theta \\ 1 + \frac{3}{2}\sin 2\theta \end{pmatrix}, \quad a_{00}^A = \begin{pmatrix} \frac{3}{16}(17\cos 4\theta - 5 + 24\sin 2\theta) \\ \frac{3}{16}(17\cos 4\theta - 5 - 24\sin 2\theta) \end{pmatrix}. \tag{4.45}$$

For the fermionic SYK$_q$ model at zero chemical potential we have $\theta = 0$ and we omit all upper subscripts A for brevity, since as we explained in (4.28) the h^S modes do not contribute to the two-point function in this case. Then $v_h = (1, 1)^T$ and also $a_{hh'} \propto (1, 1)^T$, $a_{hh'h''} \propto (1, 1)^T$, etc., and we can omit the vector notation so the coefficients $a_{hh'}$, $a_{hh'h''}$, etc., become just real numbers and thus the leading terms for the two-point function can be written as

$$G(\tau) = G^c(\tau)\left(1 - \frac{\alpha_0}{|J\tau|} - \frac{\alpha_1}{|J\tau|^{h_1-1}} - \frac{a_{00}\alpha_0^2}{|J\tau|^2} - \frac{2a_{01}\alpha_0\alpha_1}{|J\tau|^{h_1}} - \frac{a_{11}\alpha_1^2}{|J\tau|^{2h_1-2}} - \frac{a_{000}\alpha_0^3}{|J\tau|^3} + \cdots\right), \tag{4.46}$$

where $h_0 = 2$ and $h_1 \simeq 3.77$. Using (4.43) for $v_h = (1, 1)$ and $\theta = 0$, we find explicitly

$$a_{00} = \frac{(2\Delta + 1)(2 - 2\Delta - \cos 2\pi\Delta)}{8\Delta\cos^2\pi\Delta}. \tag{4.47}$$

In general, it is possible to obtain corrections up to an arbitrary order. As an example for the cubic order in α_0 the result takes the form, for $\theta = 0$,

$$a_{000} = \frac{(\Delta + 1)(2\Delta + 1)(6\Delta - 8 + \cos 2\pi\Delta)}{24\Delta^2\cos^2\pi\Delta}. \tag{4.48}$$

We checked that the results for $a_{hh'}$ and a_{000} in (4.43) and (4.48) for $\theta = 0$ exactly match with the large-q and $q \to 2$ expansions discussed in Appendixes B and C.

C. Finite-temperature generalization

The results described above are only applicable at zero temperature. To generalize to finite temperature, we use the U(1) and time-reparametrization symmetry of the conformal saddle-point equations. In the presence of the symmetry, G, Σ, W_G, and W_Σ are all covariant under time reparametrization and U(1). Therefore, the coefficients α_h should be temperature independent, and all we need is the finite-temperature form of the scaling function $\mathcal{F}_h$.

As we already discussed in Sec. III, in general, for the complex fermions with the particle-hole symmetry the three-point function has two independent structures [24,33]

$$\langle f(\tau_1)f^\dagger(\tau_2)O_h(\tau_0)\rangle$$
$$= \frac{b^\Delta\left[c_h^A\mathrm{sgn}(\tau_{12}) + c_h^S\mathrm{sgn}(\tau_{10})\mathrm{sgn}(\tau_{20})\right]}{\left|\frac{\beta J}{\pi}\sin\frac{\pi\tau_{12}}{\beta}\right|^{2\Delta-h}\left|\frac{\beta J}{\pi}\sin\frac{\pi\tau_{10}}{\beta}\right|^h\left|\frac{\beta J}{\pi}\sin\frac{\pi\tau_{20}}{\beta}\right|^h}, \tag{4.49}$$

where c_h^A and c_h^S are independent structure constants and the sign function is antiperiodic on the thermal circle $\mathrm{sgn}(\tau + \beta) = -\mathrm{sgn}(\tau)$. This form is consistent with higher-dimensional CFT results for fermions (see, for example, [34,35]) and gives correct statistics for the fermionic and bosonic fields, when one of the fields is moved over the full thermal circle. For a nonzero chemical potential this result was generalized in [22] and takes the form

$$\langle f(\tau_1)f^\dagger(\tau_2)O_h(\tau_0)\rangle$$
$$= -G_f^c(\tau_{12})\frac{c_h^A + c_h^S\mathrm{sgn}(\tau_{12})\mathrm{sgn}(\tau_{10})\mathrm{sgn}(\tau_{20})}{\left|\sin\frac{\pi\tau_{12}}{\beta}\right|^{-h}\left|\frac{\beta J}{\pi}\sin\frac{\pi\tau_{10}}{\beta}\sin\frac{\pi\tau_{20}}{\beta}\right|^h}, \tag{4.50}$$

where we used conformal Green's functions $G_f^c(\tau)$ to write the three-point function compactly. For the bosonic case we have to replace $G_f^c(\tau)$ by $G_\mathfrak{b}^c(\tau)$. For a domain $\tau \in [-\beta, \beta]$ the formulas for the conformal two-point functions are

$$G_f(\tau) = -e^{\pi\mathcal{E}_f\mathrm{sgn}(\tau)}\frac{b_f^\Delta\mathrm{sgn}(\tau)}{\left|\frac{\beta J}{\pi}\sin\frac{\pi\tau}{\beta}\right|^{2\Delta}}e^{-(2\pi/\mathcal{E}_f\beta)\tau},$$

$$G_\mathfrak{b}(\tau) = -e^{\pi\mathcal{E}_\mathfrak{b}\mathrm{sgn}(\tau)}\frac{b_\mathfrak{b}^\Delta}{\left|\frac{\beta J}{\pi}\sin\frac{\pi\tau}{\beta}\right|^{2\Delta}}e^{-(2\pi/\mathcal{E}_\mathfrak{b}\beta)\tau}. \tag{4.51}$$

The appearance of the factors $\exp(-\frac{2\pi\mathcal{E}}{\beta}\tau)$ in the three-point functions can be derived by applying the U(1) transformation on f and $f^\dagger$, assuming O_h is neutral under U(1). One can check that the expression (4.50) agrees with (3.11) upon taking the $\beta \to \infty$ limit and setting $\mathcal{E}_f = c_h^S = 0$. We also remark that the three-point functions (4.50) represent a basis for the kernel K_G. This A/S basis is related to the previously used plus/minus basis by some transformation matrix.

Analogously to the discussion in Sec. III, the linear correction to the two-point function can be computed as

$$\delta_h G(\tau_{12}) = g_h\int_0^\beta d\tau_0\langle f(\tau_1)f^\dagger(\tau_2)O_h(\tau_0)\rangle, \tag{4.52}$$

where we recall that $g_h \propto J$ is dimensionful coupling. The correction is split into two parts $\delta_h G(\tau) = \delta_h G_A(\tau) + \mathrm{sgn}(\tau)\delta_h G_S(\tau)$ and to match our result (4.24) for zero temperature we have

$$\frac{\delta_h G_A(\tau)}{G^c(\tau)} = -\frac{1}{2}(v_{h+} + v_{h-})\frac{\alpha_h}{(\beta J)^{h-1}}f_h^A(\tau),$$

$$\frac{\delta_h G_S(\tau)}{G^c(\tau)} = -\frac{1}{2}(v_{h+} - v_{h-})\frac{\alpha_h}{(\beta J)^{h-1}}f_h^S(\tau), \tag{4.53}$$

where

$$f_h^A(\tau_{12}) \propto \int_0^\beta d\tau_0\frac{\left|\sin\frac{\pi\tau_{12}}{\beta}\right|^h}{\left|\sin\frac{\pi\tau_{10}}{\beta}\sin\frac{\pi\tau_{20}}{\beta}\right|^h},$$

$$f_h^S(\tau_{12}) \propto \int_0^\beta d\tau_0\frac{\left|\sin\frac{\pi\tau_{12}}{\beta}\right|^h\mathrm{sgn}(\tau_{10})\mathrm{sgn}(\tau_{20})}{\left|\sin\frac{\pi\tau_{10}}{\beta}\sin\frac{\pi\tau_{20}}{\beta}\right|^h}. \tag{4.54}$$

The function $\mathcal{F}_h(\tau/\beta)$ defined in (4.1) reads

$$\mathcal{F}_h\left(\frac{\tau}{\beta}\right) = \frac{1}{2}(v_{h+} + v_{h-})f_h^A(\tau) + \frac{1}{2}(v_{h+} - v_{h-})f_h^S(\tau)\mathrm{sgn}(\tau). \tag{4.55}$$

Using results from [7,22] for the integrals in (4.54) and fixing proportionality constants such that $f_h^{A/S}(\tau) \to (\beta/|\tau|)^{h-1}$ in the limit $\beta \to \infty$, we obtain

$$f_h^A(\tau) = \frac{(2\pi)^{h-1}\Gamma(h)^2}{2 \sin \frac{\pi h}{2} \Gamma(2h-1)} [A_h(e^{i(2\pi\tau/\beta)}) + A_h(e^{-i(2\pi\tau/\beta)})],$$

(4.56)

$$f_h^S(\tau) = \frac{(2\pi)^{h-1}\Gamma(h)^2}{2 \cos \frac{\pi h}{2} \Gamma(2h-1)} [iA_h(e^{i(2\pi\tau/\beta)}) - iA_h(e^{-i(2\pi\tau/\beta)})],$$

(4.57)

where $A_h(u) = (1-u)^h \mathbf{F}(h, h, 1; u)$ and $\mathbf{F}$ is the regularized hypergeometric function. Our definition of A_h coincides with $A_{h,0}^{\pm}$ defined in [7,36] and we have dropped the $\pm$ notation because the two definitions in the references agree for our choice of parameter. Inside the unit circle $|u| \leqslant 1$ we can compute $A_h(u)$ using series expansion. We provide results for the $h_0^A = 2$ mode

$$f_0^A(\tau) = 2 + \frac{\pi - \frac{2\pi|\tau|}{\beta}}{\tan \frac{\pi|\tau|}{\beta}}, \quad f_0^S(\tau) = \frac{\pi}{\tan \frac{\pi|\tau|}{\beta}}.$$

(4.58)

One has to be careful computing the function $f_0^A(\tau)$ since the prefactor in (4.56) diverges and we need to expand $A_h(u)$ to the next order in h, so for $h \to 2$ we have $A_h(u) = (1 + u)/(1-u) - (h-2)[(1+u)\ln(1-u) - 2u]/(1-u) + \cdots$.

The above procedure is relatively simple for linear in α_h order. For nonlinear order the computation involves complicated products of hypergeometric functions and we leave it for future investigation.

At the end of this section we derive an expression for the spin spectral density. The spin-spin correlator in imaginary time is $Q(\tau) = -\langle \mathcal{T}_\tau(S(\tau)S(0)) \rangle$ and using that $S = f^\dagger f$ or $S = \mathfrak{b}^\dagger \mathfrak{b}$ in the large-M limit we find

$$Q(\tau) = -\zeta G(\tau)G(-\tau).$$

(5.5)

Expressing Green's function $G(\tau)$ through the spectral density and using a similar formula for $Q(\tau)$, we find the expression

V. SPECTRAL DENSITIES

To numerically study the models discussed above, it is convenient to work with spectral density $\rho(\omega)$ instead of the Green's function. For the fermionic and bosonic SYK models we define it as

$$G(i\omega_n) = \int_{-\infty}^{+\infty} d\omega \frac{\rho(\omega)}{i\omega_n - \omega}.$$

(5.1)

This definition implies that $\int_{-\infty}^{+\infty} d\omega \rho(\omega) = 1$ and the spectral density can be found as

$$\rho(\omega) = -\frac{1}{\pi} \mathrm{Im} G_R(\omega),$$

(5.2)

where $G_R(\omega)$ is the retarded Green's function. It is related to the Matsubara function $G(i\omega_n)$ by analytic continuation from the upper half complex ω plane, namely, we have $G_R(\omega) = G(i\omega_n = \omega + i0)$, where $\omega_n \geqslant 0$. Using (4.16), we find for the conformal G_R^c and ρ^c, written in the plus/minus basis,

$$G_R^c(\omega) = \frac{C}{J} \binom{e^{-i\pi\Delta - i\theta}}{-e^{i\pi\Delta - i\theta}} |\omega/J|^{2\Delta-1},$$

$$\rho^c(\omega) = \frac{C}{\pi J} \binom{\sin(\pi\Delta + \theta)}{\sin(\pi\Delta - \theta)} |\omega/J|^{2\Delta-1}.$$

(5.3)

Next, using the Fourier transform (4.37) for Eq. (4.44) and making analytical continuation to the real frequencies, we find the general formula for the retarded Green's function. Then using the formula (5.2), we obtain the expansion of the spectral density at low frequencies

$$\rho(\omega) = \rho^c(\omega) \left(1 - \sum_h \frac{\Gamma(2\Delta)\alpha_h v_h |\omega/J|^{h-1}}{\Gamma(2\Delta + h - 1)} - \sum_{h,h'} \frac{\Gamma(2\Delta)\alpha_h \alpha_{h'} a_{hh'} |\omega/J|^{h+h'-2}}{\Gamma(2\Delta + h + h' - 2)} - \cdots \right).$$

(5.4)

for the spin spectral density

$$\rho_Q(\omega) = \int_{-\infty}^{\infty} d\nu \, \rho(\nu)\rho(\nu - \omega)[n(\nu - \omega) - n(\nu)], \quad (5.6)$$

where $n(\omega) = 1/(e^{\beta\omega} - \zeta)$ is the Fermi or Bose distribution. At zero temperature we have $n(\omega) = -\zeta\theta(-\omega)$ and we obtain

$$\rho_Q(\omega) = -\zeta \int_0^\omega d\nu \, \rho(\nu)\rho(\nu - \omega),$$

(5.7)

which is valid for both positive and negative frequencies ω. Using (5.3) and (5.4), we find

$$\rho_Q(\omega) = \rho_Q^c(\omega) \left(1 - \sum_h \frac{\Gamma(4\Delta)\alpha_h (v_{h+} + v_{h-})|\omega/J|^{h-1}}{\Gamma(4\Delta + h - 1)} - \sum_{h,h'} \frac{\Gamma(4\Delta)\alpha_h \alpha_{h'} (a_{hh'+} + a_{hh'-} - v_{h+}v_{h'-})|\omega/J|^{h+h'-2}}{\Gamma(4\Delta + h + h' - 2)} - \cdots \right)$$

(5.8)

and the conformal spin spectral density is

$$\rho_Q^c(\omega) = \mathrm{sgn}(\omega) \frac{b^{2\Delta}}{J\Gamma(4\Delta)} |\omega/J|^{4\Delta-1}.$$

(5.9)

For comparison to numerical results, we can find for the $q = 4$ fermionic SYK model at $\theta_f = 0$ that the first few terms in ρ_{Q_f} for $\omega > 0$ are

$$\rho_{Q_f}(\omega) = \rho_{Q_f}^c(\omega)\left[1 - 2\alpha_0^A\left(\frac{\omega}{J}\right) - \frac{7}{4}(\alpha_0^A)^2\left(\frac{\omega}{J}\right)^2 - 0.44\alpha_1^A\left(\frac{\omega}{J}\right)^{2.77} + \frac{37}{6}(\alpha_0^A)^3\left(\frac{\omega}{J}\right)^3 + \cdots\right], \quad (5.10)$$

where we used values of a_{00} and a_{000} from (4.47) and (4.48) and $h_1^A \simeq 3.77$.

We generalize results for the spectral densities at finite temperature in Appendix D. Here we only present a finite-temperature generalization of Eq. (5.8) for $\Delta = 1/4$, where only the $h_0^A = 2$ mode is retained,

$$\rho_Q(\omega) = \frac{b^{1/2}}{J}\tanh\left(\frac{\beta\omega}{2}\right)\left[1 - \frac{2\alpha_0^A\omega}{J}\tanh\left(\frac{\beta\omega}{2}\right) - \cdots\right], \quad (5.11)$$

and we used that $v_{0+} + v_{0-} = 2$. The coefficient of the correction term $2\alpha_0^A/J$ can be related to the coefficient γ in specific heat $C = \gamma T$ by the Schwarzian action argument in [22], with the result

$$\mathcal{C}_f = \frac{2\alpha_0^A/J}{\gamma} = \frac{24}{\pi[2\cos 2\theta_f + 3\pi\cos^2 2\theta_f]}. \quad (5.12)$$

For bosonic spinon theory, there is an extra minus sign because bosonic action differs from the fermionic version by a minus sign:

$$\mathcal{C}_\mathfrak{b} = \frac{2\alpha_0^A/J}{\gamma} = -\frac{24}{\pi[2\cos 2\theta_\mathfrak{b} + 3\pi\cos^2 2\theta_\mathfrak{b}]}. \quad (5.13)$$

VI. RANDOM QUANTUM ROTOR MODEL

In this section we consider the random quantum q-rotor model (also known as the quantum spherical q-spin model), where q is a positive integer number. The Hamiltonian of this model has the form

$$H = \sum_{i=1}^N \frac{\pi_i^2}{2M} + \sum_{i_1,\ldots,i_q}^N J_{i_1,\ldots,i_q}\phi_{i_1},\ldots,\phi_{i_q}, \quad (6.1)$$

where M is the mass, π_i is the conjugate momentum to a real scalar spin variable ϕ_i so $[\phi_i, \pi_j] = i\delta_{ij}$, and there is the spherical constraint $1/N\sum_{i=1}^N\langle\phi_i^2\rangle = 1$. The couplings $J_{i_1,\ldots,i_q}$ are independent Gaussian variables with zero mean and variance

$$\overline{J_{i_1,\ldots,i_q}^2} = \frac{\tilde{J}^2}{qN^{q-1}}. \quad (6.2)$$

This model was first studied in [37,38] and similar models were considered in [39–43]. We define the imaginary-time Green's function at finite temperature

$$G(\tau) = \frac{1}{N}\sum_{i=1}^N\langle\mathcal{T}_\tau(\phi_i(\tau)\phi_i(0))\rangle. \quad (6.3)$$

Introducing replicas and averaging over disorder, it is possible to derive Schwinger-Dyson equations for the function $G(\tau)$ in the large-N limit

$$G(i\omega_n) = \frac{1}{\omega_n^2 + \lambda - \Sigma(i\omega_n)}, \quad \Sigma(\tau) = J^2 G(\tau)^{q-1}, \quad (6.4)$$

where $\omega_n = 2\pi n/\beta$ are Matsubara frequencies and λ is the Lagrange multiplier imposing the spherical constraint. Also, we assumed a replica symmetric solution and made the rescaling $\phi \to \phi/\sqrt{M}$, so the spherical constraint takes the form $G(\tau = 0) = M$ and also $J = \tilde{J}/M^{q/2}$. Similarly to the SYK models, Eqs. (6.4) admit a conformal solution in the IR region for a given J upon tuning M and thus λ to a critical value. The conformal solution reads

$$G^c(\tau) = \frac{b^\Delta}{|(\beta J/\pi)\sin(\pi\tau/\beta)|^{2\Delta}}, \quad (6.5)$$

where $\Delta = 1/q$ and dimensionless constant b coincides with $b_\mathfrak{b}$ in (2.17) computed for $\theta_\mathfrak{b} = \pi/2$. The analysis from Sec. IV can be applied to the random rotor model. The only difference is that the source term now is $\sigma(\tau) = \partial_\tau^2$. The correction to the conformal Green's function comes from $h^A(\theta)$ modes computed at $\theta_\mathfrak{b} = \pi/2$. For $q = 4$ these modes are represented by blue lines in Fig. 3 and for $\theta_\mathfrak{b} = \pi/2$ we find $h_0^A = 2$, $h_1^A \simeq 4.26$, $h_2^A \simeq 6.34$, etc. Symmetric modes h^S do not contribute to the two-point function due to the exact particle-hole symmetry [see the discussion around Eq. (4.28)]. We note that for $\theta_\mathfrak{b} = \pi/2$ there is a complex mode in the symmetric sector [40]. Though the complex mode formally does not affect the large-N two-point function, it presumably makes the replica diagonal solution unstable and leads to replica symmetry breaking. We also remark that the appearance of the complex modes in some non-Fermi-liquid theories was noticed in [44]. In any case it is interesting to study the conformal solution of the Schwinger-Dyson Eqs. (6.4). The leading analytical corrections to the Green's function at zero temperature read

$$G(\tau) = G^c(\tau)\left(1 - \frac{\alpha_0}{|J\tau|} - \frac{a_{00}\alpha_0^2}{|J\tau|^2} - \frac{a_{000}\alpha_0^3}{|J\tau|^3} - \frac{\alpha_1}{|J\tau|^{h_1-1}} - \cdots\right), \quad (6.6)$$

where we omitted subscripts A for brevity and for $q = 4$ we find $a_{00} = 9/4$ and $a_{000} = -65/4$ from (4.47) and (4.48), which are also valid for $\theta_\mathfrak{b} = \pi/2$ and $\Delta = 1/4$. We note that in this case quadratic and cubic nonlinear terms of the $h_0 = 2$ mode are more dominant than the linear correction of the h_1 mode. In Sec. VII we will verify (6.6) numerically for $q = 4$ by computing the spectral density at zero temperature. The spectral density $\rho(\omega)$ is defined as

$$G(i\omega_n) = \int_{-\infty}^{+\infty} d\omega\, \frac{\rho(\omega)}{\omega - i\omega_n}, \quad (6.7)$$

and due to the particle-hole symmetry the spectral density is an odd function $\rho(-\omega) = -\rho(\omega)$. Using this we can write (6.7) in the form

$$G(i\omega_n) = \int_{-\infty}^{+\infty} d\omega\, \frac{\omega\rho(\omega)}{\omega^2 + \omega_n^2}, \quad (6.8)$$

and taking the large-z limit we find $\int_{-\infty}^{+\infty} d\omega\, \omega\, \rho(\omega) = 1$. We also note that unitarity implies that $\rho(\omega) > 0$ for $\omega > 0$. We will find numerically that $\alpha_0 \simeq -0.556$ for the $q = 4$ case. We note that it is negative, whereas for bosonic and fermionic SYK models α_0 is positive.

VII. NUMERICAL RESULTS FOR SPINON SPECTRA

In this section we present numerical solutions of the real-time Schwinger-Dyson equations at zero temperature for the bosonic and fermionic spinon models and also the random rotor model in the case of $q = 4$. We study the corrections found analytically in Sec. IV and provide numerical evidence that the conformal solutions and the corrections to the conformal solutions work very well for all parameters in the fermionic model and for some range of parameters in the bosonic model. We also numerically find values of the dimensionless coefficients α_h for the first terms in the sum (5.4) for a range of asymmetry angles θ_f and θ_b and argue that the numerically found spectra of operators agree with the ones found analytically.

The first Schwinger-Dyson equation for bosonic and fermionic spinon models is

$$G_R(\omega)^{-1} = \omega + i0 + \mu - \Sigma_R(\omega), \qquad (7.1)$$

and using the second Schwinger-Dyson equation we can express the retarded self-energy $\Sigma_R(\omega)$ though the spectral density $\rho(\omega)$, which is in turn related to $G_R(\omega)$ as $\rho(\omega) = -\frac{1}{\pi}\text{Im}G_R(\omega)$. We solve these equations at zero temperature

using iterations. The detailed derivation of the equations above and numerical technique is discussed in Appendix E and we note that a similar numerical approach was used in [1].

At zero temperature we expect the spectral density to diverge at small frequencies; therefore, the quantity of interest is

$$\rho(\omega) = \begin{cases} \dfrac{g_+(\omega)}{\sqrt{\omega/J}}, & \omega > 0 \\[2mm] \dfrac{g_-(-\omega)}{\sqrt{-\omega/J}}, & \omega < 0. \end{cases} \qquad (7.2)$$

We are interested in finding a solution of the SD equations that at zero frequency approaches the conformal solution. Therefore, the function of interest $g_\pm(\omega)$ should approach a constant

$$g_\pm(0) = \frac{C}{\pi J}\sin(\pi/4 \pm \theta), \quad C = \left(\frac{-\zeta\pi}{\cos 2\theta}\right)^{1/4} \qquad (7.3)$$

according to Eqs. (5.3) and (5.4). We remark that these boundary conditions at $\omega = 0$ determine the asymmetry angle θ of the numerical solution and the chemical potential is fixed to be $\mu = \Sigma_R(0)$ and is not an input parameter at zero-temperature numerics. In contrast, for the finite-temperature numerics one fixes μ first and then can infer θ by analyzing the numerical solution.

We are interested in the low-frequency behavior of the numerical solution that is described theoretically in Sec. IV for both fermionic and bosonic spinon models. We use the expansion of the spectral density at small frequencies (5.4) and rewrite the expression at $\Delta = 1/q = 1/4$ for the function $g_\pm(\omega)$ as

$$g_\pm(\omega) = g_\pm(0)\left(1 - \sum_h \frac{\sqrt{\pi}\,\alpha_h v_{h\pm}(\omega/J)^{h-1}}{\Gamma(h - 1/2)} - \sum_{h,h'} \frac{\sqrt{\pi}\,\alpha_h \alpha_{h'} a_{hh'\pm}(\omega/J)^{h+h'-2}}{\Gamma(h + h' - 3/2)} - \cdots\right), \qquad (7.4)$$

where $g_\pm(0)$ is given in (7.3). The coefficients α_h depend on asymmetry angles θ_f and θ_b and are different for fermionic and bosonic models. The eigenvectors $v_h = (v_{h+}, v_{h-})$ of the matrix K_G and vectors $a_{hh'}, a_{hh'h''}, \ldots$ also depend on the asymmetry angles and are given by Eqs. (4.25) and (4.43). For a given asymmetry angle there are first few leading modes in (7.4) which dominate the low-frequency expansion.

Let us start with the fermionic SYK model at zero chemical potential. In this case $\theta_f = 0$ and due to particle-hole symmetry all h^S modes do not contribute. Also, $g_+ = g_- = g$ and the leading terms in (7.4) are

$$g_f(\omega) = \frac{1}{(4\pi^3)^{1/4}J}\left[1 - 2\alpha_0^A\frac{\omega}{J} - 3(\alpha_0^A)^2\left(\frac{\omega}{J}\right)^2 - 0.68\alpha_1^A\left(\frac{\omega}{J}\right)^{2.77} + \frac{26}{3}(\alpha_0^A)^3\left(\frac{\omega}{J}\right)^3 - \cdots\right], \qquad (7.5)$$

where we used that $v_h^A = (1, 1)$ and $h_1^A \simeq 3.77$ and also $a_{00}^A = 9/4$ and $a_{000}^A = -65/4$ [see Eqs. (4.47) and (4.48)] for $\Delta = 1/4$ and $\theta_f = 0$. Fitting numerical data, we can find $\alpha_0^A = 0.2643$ and $\alpha_1^A \simeq 0.31$–0.36. We plot the numerical result and theory (7.5) in Fig. 4. We can see really good agreement between theory and numerics at low frequencies. We note that since the α_1^A term is subleading we cannot fix it with good precision. In contrast, α_0^A can be fixed with high accuracy and our result agrees well with previous computation of this term in [6].

For nonzero chemical potential and thus nonzero asymmetry angle θ_f modes from the symmetric sector contribute to the spectral density and since $h_1^S < 3$ the leading terms in low-frequency expansion of $g_\pm(\omega)$ are

$$g_{f\pm}(\omega) = \frac{\sin(\frac{\pi}{4} \pm \theta_f)}{J(\pi^3\cos 2\theta_f)^{1/4}}\left[1 - 2\alpha_0^A v_{0\pm}^A\frac{\omega}{J} - \frac{\sqrt{\pi}\alpha_1^S v_{1\pm}^S}{\Gamma(h_1^S - \frac{1}{2})}\left(\frac{\omega}{J}\right)^{h_1^S - 1} - \frac{4}{3}(\alpha_0^A)^2 a_{00\pm}^A\left(\frac{\omega}{J}\right)^2 - \cdots\right], \qquad (7.6)$$

where explicit expressions for the vectors v_0^A and a_{00}^A are given in (4.45) and the vector v_1^S can be computed from (4.25)

for a given value of h_1^S. The θ_f angle dependence of h_1^S is represented in Fig. 3.
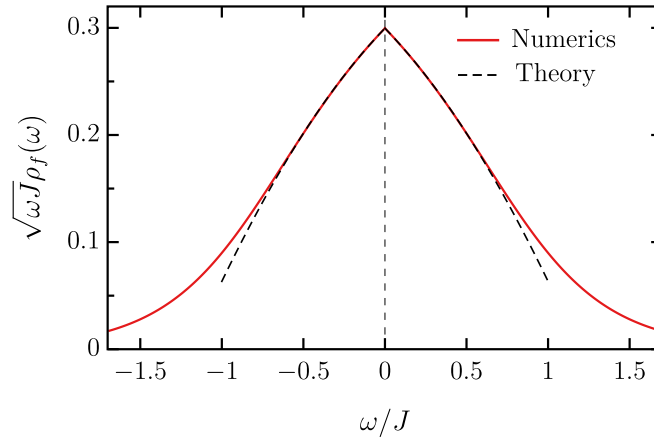
FIG. 4. Plot of the fermionic SYK$_4$ spectral density for $\theta_f = 0$ at zero temperature. The red solid line is the numerical result obtained by solving the Schwinger-Dyson equations using iterations. The black dashed line is the theoretical curve (7.5) plotted for $\alpha_0^A = 0.2643$ and $\alpha_1^A = 0.31$.

We remark that since the series (7.4) is asymptotic[3] the relevance of higher-order terms depends on the range of $\omega \in [0, \omega_{max}]$ for which we approximate the exact result. This means that if we truncate the series at order p_{max} the maximal frequency ω_{max} for which this series gives a reasonable approximation to the exact result is roughly determined by the condition that the term $(\omega_{max}/J)^{p_{max}}$ becomes comparable to the lower-order terms in the series. Based on this and approximate values of the coefficients α_h for the fermionic SYK$_4$ model, we keep only two or three leading terms written in (7.6).

We also notice that the coefficient α_0^A can be found by fitting the numerical curve by the linear correction

$$g_\pm^{lin}(\omega) = g_\pm(0)\left[1 - 2\alpha_0^A\left(1 \mp \frac{3}{2}\sin 2\theta_a\right)\frac{\omega}{J}\right]. \quad (7.7)$$

We present the solutions of Eqs. (E7)–(E13) and the corresponding fitting of the analytical formula (7.6) in Fig. 5 for the fermionic spinon model and in Fig. 6 for the bosonic spinon model.

For the bosonic case the two leading operators are $h_0^A = 2$ and h_1^A; therefore, we have

$$g_{\mathfrak{b}\pm}(\omega) = \frac{\sin\left(\frac{\pi}{4} \pm \theta_{\mathfrak{b}}\right)}{J(-\pi^3\cos 2\theta_{\mathfrak{b}})^{1/4}}\left[1 - 2\alpha_0^A v_{0\pm}^A\frac{\omega}{J} - \frac{\sqrt{\pi}\alpha_1^A v_{1\pm}^A}{\Gamma\left(h_1^A - \frac{1}{2}\right)}\left(\frac{\omega}{J}\right)^{h_1^A - 1} - \frac{4}{3}\left(\alpha_0^A\right)^2 a_{00\pm}^A\left(\frac{\omega}{J}\right)^2 - \frac{2\sqrt{\pi}\alpha_0^A\alpha_1^A a_{01\pm}^A}{\Gamma\left(h_1^A + \frac{1}{2}\right)}\left(\frac{\omega}{J}\right)^{h_1^A}\right.$$

$$\left. - \frac{\sqrt{\pi}\left(\alpha_1^A\right)^2 a_{11\pm}^A}{\Gamma\left(2h_1^A - \frac{3}{2}\right)}\left(\frac{\omega}{J}\right)^{2h_1^A - 2} - \cdots\right]. \quad (7.8)$$

For $\theta_{\mathfrak{b}} > 0.284\pi$ the anomalous dimension h_1^A becomes less than $h_0^A = 2$ and thus starts dominating the expansion in (7.8).

The numerical approach we use in this section allows us to compute the coefficients α_h in the formula (7.6) with very good precision. We use the function (7.6) as a fitting polynomial and find the dimensionless coefficients of each term. The results for the fermionic case are presented in Fig. 7 and for the bosonic case in Fig. 8. For the bosonic model, we see that the value of α_h becomes very large at some value of $\theta_{\mathfrak{b}}$. This value is close to $\theta_{\mathfrak{b}} = 0.284\pi$ where $h_0^A = h_1^A$ and $k_A'(h) = 0$. We do not include the region where $h_1^A \leqslant h_0^S = 1$ since the numerical solution is not described by the conformal theory and is probably nonphysical.

Even though the coefficients α_h cannot be computed analytically as discussed in Sec. IV, and therefore the fitting

functions cannot be exactly determined and has to include numerical results, there are ways to understand how well numerical solutions work by comparing them with pure theoretical predictions. One way to do this is to compute the ratio of coefficients in front of each term in (7.6). The general formula of the ratio of each term reads

$$r_h(\theta_a) = \frac{\sin(\pi\Delta - \theta_a)}{\sin(\pi\Delta + \theta_a)}\frac{v_{h_-}}{v_{h_+}}, \quad (7.9)$$

where v_h are the eigenvectors found in Sec. IV; therefore, $v_{h\pm}$ are the components of the eigenvector that correspond to the positive and negative frequencies. We can compute this ratio both analytically and numerically (using the analytically found resonance values of h). The results of the first two terms are presented in Fig. 9 for the fermionic and bosonic models. We again note that for the bosonic model we do not include the region where h_1^A becomes less than one, since we cannot trust the solution in this region.

---

[3]This can be seen from the $q = 2$ case, where the explicit formula (C1) for $G(\tau)$ is available.
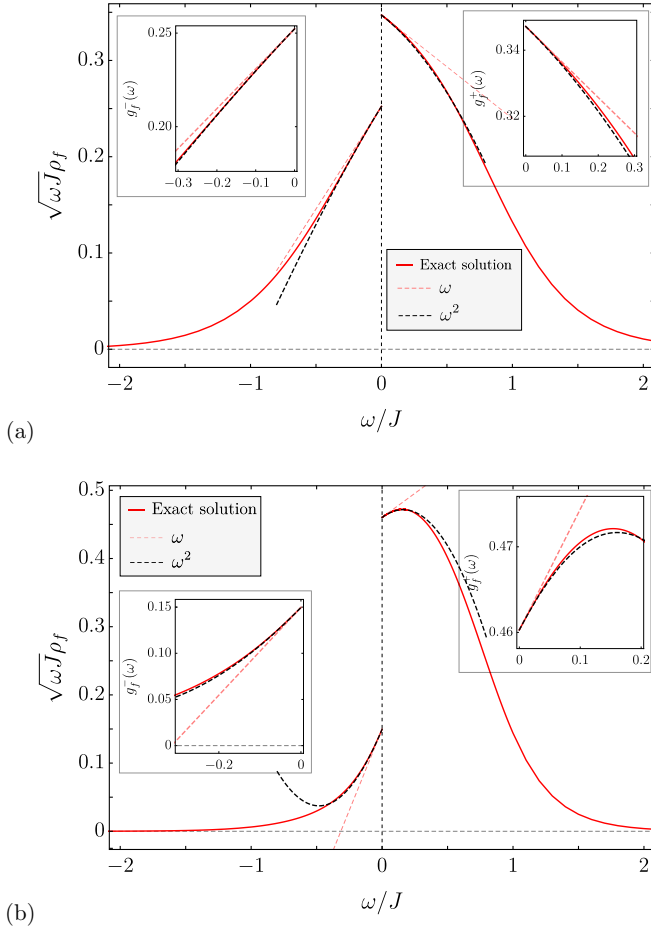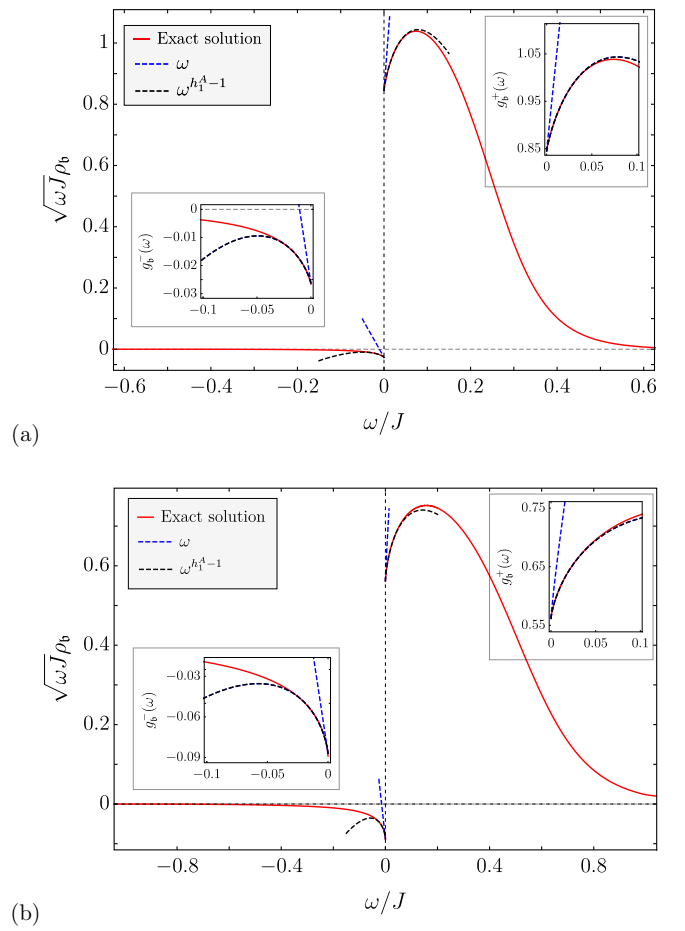
FIG. 5. Spectral density plots at zero temperature for the fermionic spinon model. The red solid lines are the numerical solution of Eqs. (E7)–(E13) for the fermionic case at the value of the asymmetry parameter (a) $\theta_f = 0.05\pi$ and (b) $\theta_f = 0.15\pi$. The dashed lines are the fitting given by theoretical formula (7.6). The pink dashed lines are the linear fit given by (7.7) with (a) $\alpha_0^A \simeq$ 0.29 and (b) $\alpha_0 \simeq 0.68$. The black dashed lines are the fitting with the first four terms (nonlinear fitting is included) $g_\pm(\omega) = g_\pm(0)(1 + a\omega + b\omega^{h_1^S - 1} + c\omega^2)$, where c is a coefficient that depends on α_0^S and (a) $h_1^S \simeq 2.63$ and $\alpha_1^S \simeq 0.05$ and (b) $h_1^S \simeq 2.53$ and $\alpha_1^S \simeq 0.06$. The insets show close-ups of $g_f^\pm$ at small frequencies. The legend shows the powers of frequencies at which the series is terminated.

Another way to compare the numerical and theoretical results is to compute the Luttinger relations (4.27) for both models. Numerically, we find $Q(\theta_f)$ and $S(\theta_\mathfrak{b})$ from the spectral density at zero temperature as $S = -\int_{-\infty}^0 d\omega\, \rho_\mathfrak{b}(\omega)$ and $Q = \int_0^\infty d\omega\, \rho_f(\omega) - 1/2$ and compare them with the theory. The results for both models are presented in Fig. 10. We note that both solutions are close to the theoretical curves within $\Delta S, \Delta Q \sim 10^{-6}$ for each numerical point. As it was discussed in Sec. IV A, at the asymmetry angle $\theta_\mathfrak{b} \simeq 0.36\pi$ where the anomalous dimension $h_1^A \lessgtr 1$ for the bosonic model, the Luttinger relation stops working. As we can see in Fig. 10(a), this indeed happens around $\theta_\mathfrak{b} \simeq 0.36\pi$, as predicted from the theory. It is unclear if solutions for angles $\theta_\mathfrak{b} > 0.36\pi$ are physical. Also, one can provide a general argument why

FIG. 6. Spectral density plots at zero temperature for the bosonic spinon model. The red solid lines are the numerical solution of Eqs. (E7)–(E13) for the bosonic case at the value of the asymmetry parameter (a) $\theta_\mathfrak{b} = 0.26\pi$ and (b) $\theta_\mathfrak{b} = 0.3\pi$. The dashed lines are the fitting given by (7.6). The blue dashed line is the linear fit given by (7.7) with (a) $\alpha_0^A \simeq 21.9$ and (b) $\alpha_0^A \simeq 17.3$. The black dashed lines are the fitting of the function (7.6) with the first three terms $g_\pm(\omega) = g_\pm(0)(1 + a\omega + b\omega^{h_1^A - 1})$ with (a) $h_1^A = 2.16$ and $\alpha_1^A \simeq -12.2$ and (b) $h_1^A = 1.87$ and $\alpha_1^A \simeq -8.5$. The insets show close-ups of $g_{\mathfrak{b}\pm}$ at small frequencies.

there is no conformal solution of the bosonic SYK model at $\theta_\mathfrak{b} = \pi/2$. For the conformal solution at this angle we have $S = -\int_{-\infty}^0 d\omega\, \rho_\mathfrak{b}(\omega) = 0$ and thus from unitarity $\rho_\mathfrak{b}(\omega) \leqslant 0$ for $\omega < 0$ we should conclude that $\rho_\mathfrak{b}(\omega) = 0$ for $\omega < 0$, but the conformal solution implies that $g_-(0) = -1/(4\pi^3)^{1/4}J$ at $\theta_\mathfrak{b} = \pi/2$.

It is also instructive to find values of the charge Q and spin S as a function of the chemical potentials μ_f and $\mu_\mathfrak{b}$, respectively, rather than the asymmetry angles θ_f and $\theta_\mathfrak{b}$. Numerically, we compute μ using that $\mu = \mathrm{Re}\,\Sigma_R(\omega = 0)$ and the Kramers-Kronig relation

$$\mu = \int_{-\infty}^{+\infty} \frac{d\nu}{\pi} \frac{\mathrm{Im}[\Sigma_R(\nu) - \Sigma_R(0)]}{\nu}. \tag{7.10}$$

A plot of the charge Q as a function of μ_f for the fermionic SYK model is shown in Fig. 11(a) and we see that there is a maximum absolute value of the chemical potential $|\mu_{f\,\mathrm{max}}| \simeq$
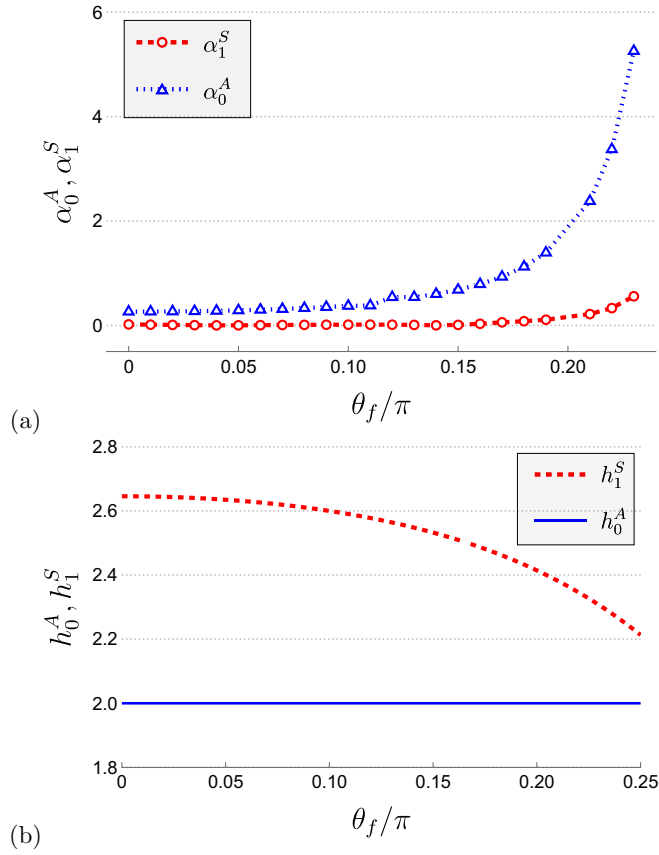
FIG. 7. Numerically computed coefficients α_h (7.6) and theoretical values of the anomalous dimension of the operator $\mathcal{O}_{h_1^S}$ in the fermionic SYK model. (a) The red circles are the numerical values of α_1^S, the coefficient due to the new operator with the anomalous dimension h_1^S, computed at different θ_f parameters; blue triangles are the numerical values of the coefficient α_0^A representing the linear correction, computed at different θ_f parameters. The lines are the linear interpolation between points. (b) The red dashed line is the plot of h_1^S given by the theoretical prediction, as a function of θ_f. The blue line is $h_0^A = 2$.

0.245J. At this value $|Q_{\max}| \simeq 0.358$. A similar dependence of Q as a function of μ_f was found in [45–47]. In [45,46] a general phase diagram in (T, μ_f) space was investigated. It was shown that at $T = 0$ the SYK solution becomes unstable already when $Q \gtrsim 0.26$ and there is a first-order phase transition to a low-entropy phase. In Fig. 11(b) we plot compressibility $K = dQ/d\mu_f$ as a function of Q. We see that it diverges at $Q_{\max}$. For the bosonic SYK case we plot $\theta_\flat$ as a function of $\mu_\flat$ in Fig. 12.

Finally, for the random quantum rotor model discussed in Sec. VI we use the expansion

$$g_\pm(\omega) = \pm \frac{1}{(4\pi^3)^{1/4}J} \left[1 - 2\alpha_0^A \frac{\omega}{J} - 3(\alpha_0^A)^2 \left(\frac{\omega}{J}\right)^2 \right.$$
$$\left. + \frac{26}{3} (\alpha_0^A)^3 \left(\frac{\omega}{J}\right)^3 - \cdots \right]. \tag{7.11}$$

We plot the numerical result and analytical fit in Fig. 13. For the fit we used only two leading terms ω and ω^2. As we mentioned at the end of Sec. VI, in this case the value
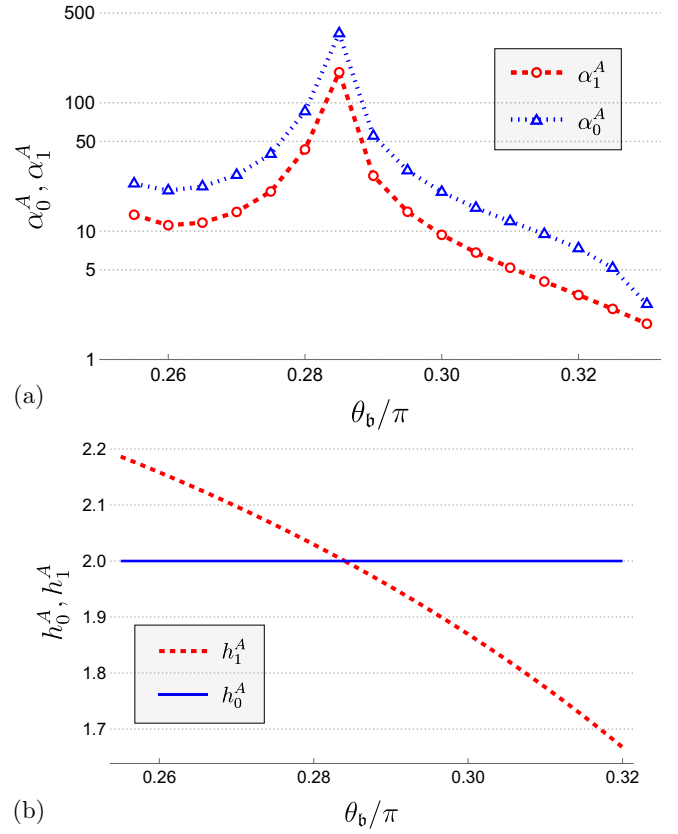
FIG. 8. (a) Numerically computed coefficients (absolute values) α_h and (b) analytical values of the anomalous dimension of the operator $\mathcal{O}_{h_1^A}$ in the bosonic SYK model. This figure is the same as Fig. 7 except the plot in (a) is in logarithmic scale. In the bosonic SYK case we notice that $h_1^A = h_0^A$ at $\theta_\flat \simeq 0.284\pi$. Near this value, the peak in (a) becomes prominent.

of $\alpha_0^A \simeq -0.556$ is negative. We also found that $M_{\text{crit}} = \int_0^{+\infty} d\omega \, \rho(\omega) \simeq 0.88$ and we checked that $\int_{-\infty}^{+\infty} d\omega \, \omega \, \rho(\omega) = 0.9988$, which confirms the validity of the numerical solution.

We conclude this section by finding numerically the spin-spin spectral density $\rho_{Q_a}(\omega)$ using the spectral density representation (7.2) in (5.7). Changing variables in order to eliminate divergences of the integrand, we find a formula suitable for numerical evaluation

$$\rho_Q(\omega) = 2 \, \text{sgn}(\omega) \int_0^{1/\sqrt{2}} \frac{dx}{\sqrt{1-x^2}} [g_+(|\omega|x^2) g_-(|\omega|(1-x^2))$$
$$+ g_-(|\omega|x^2) g_+(|\omega|(1-x^2))]. \tag{7.12}$$

For the fermionic SYK model at $\theta_f = 0$ we plot both the numerical solution and analytical formula for the spin-spin spectral density in Fig. 14, where for the black dashed line we used the analytical formula (5.10) with $\alpha_0^A \simeq 0.2643$ and $\alpha_1^A \simeq 0.31$. We note that the analytical fitting works very well at some range of frequencies where $\omega < 1$. Numerical solutions for the spin-spin spectral densities for both fermionic and bosonic spinon models for various asymmetry angles θ_f and $\theta_\flat$ without the theoretical fitting are presented in Fig. 15.
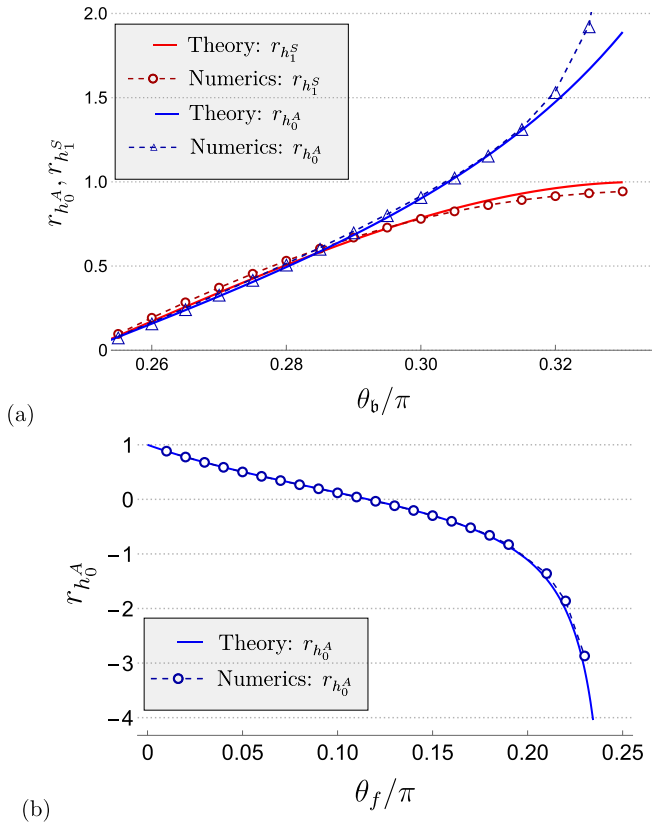
(a)

(b)

FIG. 9. Plot of the function $r_h(\theta)$ defined in (7.9) for the bosonic and fermionic models. The blue and red solid lines are analytical relations of the coefficients of the positive and negative frequencies due to the $h_0^A = 2$ and h_1^A terms, respectively, and are given by the relation (7.9). (a) The red circles and blue triangles are numerical relations $r_{h_0^A}(\theta_{\flat})$ and $r_{h_1^A}(\theta_{\flat})$, respectively. (b) The blue circles are the numerical relation $r_{h_0^A}$ at different $\theta_{\flat}$. In both panels, for the numerical fitting, we use $\omega_{max} = 7 \times 10^{-3}$ to obtain a result closest to the theory.

VIII. CONCLUSION

The SYK Eqs. (2.13) describe the large-N limit of the SYK models and the large-N limit followed by the large-M limit of the SU(M) spin models described in Sec. II. Despite their apparent simplicity, these equations contain a great deal of subtle scaling structure, which we have reviewed and extended here. The predictions of the conformal perturbation theory agree very well with the real-frequency numerical analyses, including the cases with particle-hole asymmetry. Thus the low-frequency behavior of the solutions of (2.13) can be declared to be well understood. Specifically, we have confirmed the Luttinger relations between the spectral asymmetry and the density and we have shown that the low-frequency corrections to the spectral density are controlled by the leading irrelevant operators, the most important of which is the time-reparametrization operator.

All the analysis of the present paper is at $N = \infty$, and many other works [6,7,48–51] have addressed the nature of the $1/N$ corrections to the SYK saddle point. These are dominated by the fluctuations of a quantum graviton associated with the time-reparametrization mode, which leads to a breakdown
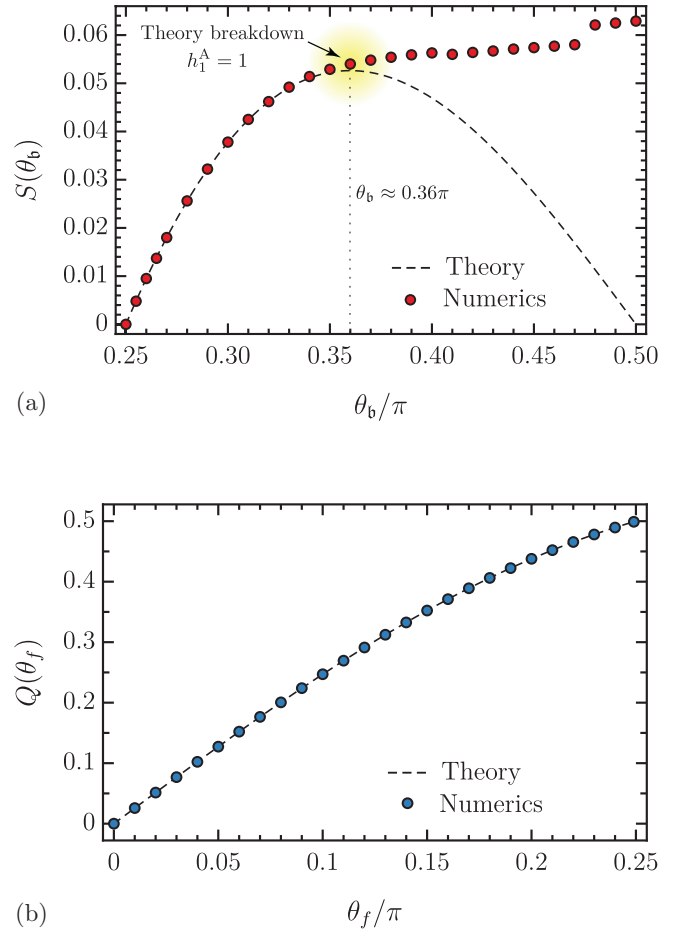

(a)

(b)

FIG. 10. Plot of (a) S as a function of $\theta_{\flat}$ for the bosonic model and (b) Q as a function of θ_f for the fermionic model. The dashed lines are given by the relations (4.27) and the red and blue points are obtained from the numerical solution for the spectral density at zero temperature. For the bosonic case we see that the numerics deviates from theory at $\theta_{\flat} \simeq 0.36\pi$, which is the angle after which the anomalous dimension h_1^A is less than 1 and thus corresponds to relevant perturbation.

of the conformal invariance described here at energy scales lower than J/N. We expect this breakdown to also apply to the SU(M) spin models.

From the condensed matter standpoint, it will be worthwhile to address the $1/M$ fluctuations of the SU(M) magnets in the $N = \infty$ theory. Upon considering the SYK model as a dynamic mean-field theory of correlated electrons, the $1/N$ corrections are finite-size corrections which are not of interest in the thermodynamic limit. On the other hand, physical systems usually have only an SU(2) symmetry, and so the $1/M$ corrections are of greater interest. We expect that the conformal structure is preserved in the $1/M$ expansion, and the "protected" scaling dimensions of the time-reparametrization mode ($h_0^A = 2$) and of the U(1) gauge symmetry mode ($h_0^S = 1$) hold to all orders in $1/M$. Renormalization group computations [21,52,53] have been used to argue that the gauge-invariant spin operator also has a protected scaling dimension and so none of the exponents in (1.2) will be modified in the $1/M$ expansion. It would be of interest to
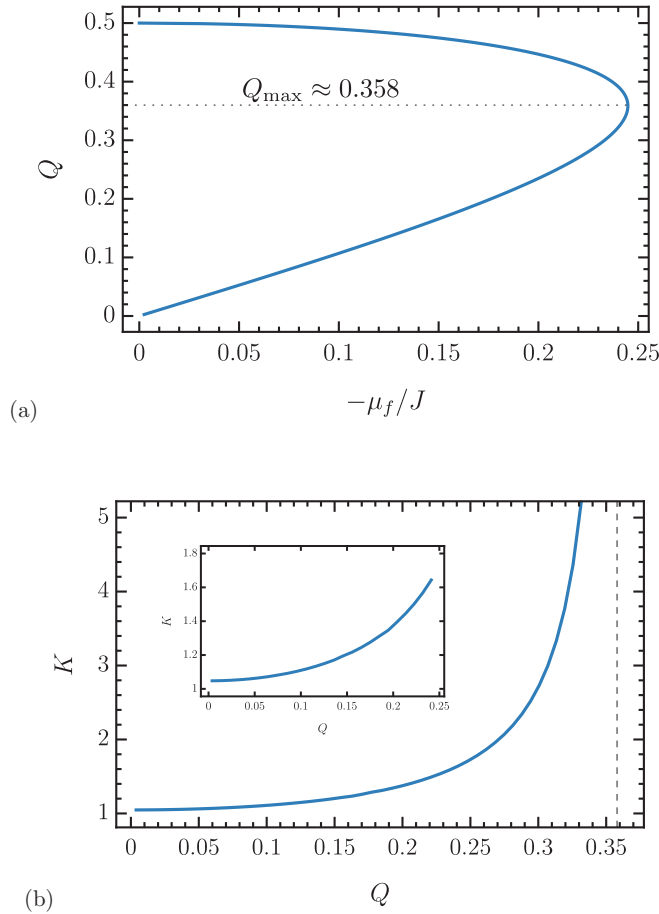
(a)

(b)

FIG. 11. (a) Charge Q as a function of the chemical potential for the fermionic SYK model at zero temperature. The blue line is the numerical solution of the Schwinger-Dyson Eqs. (E7)–(E13) for the fermionic SYK model at zero temperature for different values of the asymmetry angle. There is a maximal value of the chemical potential at which the value of the charge $Q_{max} \simeq 0.358$. (b) Compressibility K as a function of charge Q for the fermionic spinon model at zero temperature (here we set $J = 1$). Compressibility diverges at $Q_{max} \simeq 0.358$ ($\theta_f \simeq 0.153\pi$). The inset shows compressibility growth as small Q.
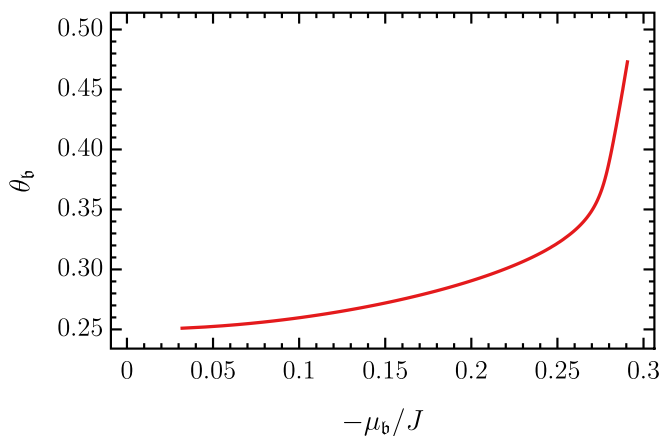
FIG. 12. Asymmetry angle $\theta_\mathfrak{b}$ as a function of the chemical potential for the bosonic SYK model at zero temperature.
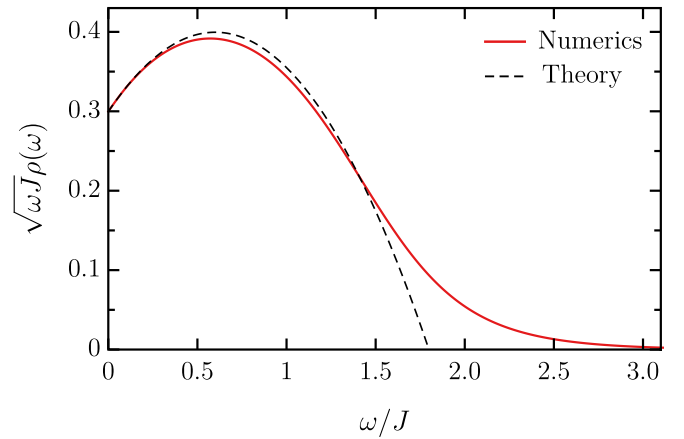

FIG. 13. Plot of the spectral density at zero temperature for the random quantum $q = 4$ rotor model. The red solid line is the numerical result obtained by solving the Schwinger-Dyson equations using iterations. The black dashed line is the analytical curve (7.11) with only two leading terms ω and ω^2 plotted for $\alpha_0^A = -0.556$.

examine these conclusions directly in the $1/M$ expansion and also determine the scaling dimensions of other possible gauge-invariant operators.

Finally, we note that we have extended the analysis of the present paper to the doped magnet, described by the SU(M) t-J model studied in Ref. [21]. These results are described in the following paper [20].
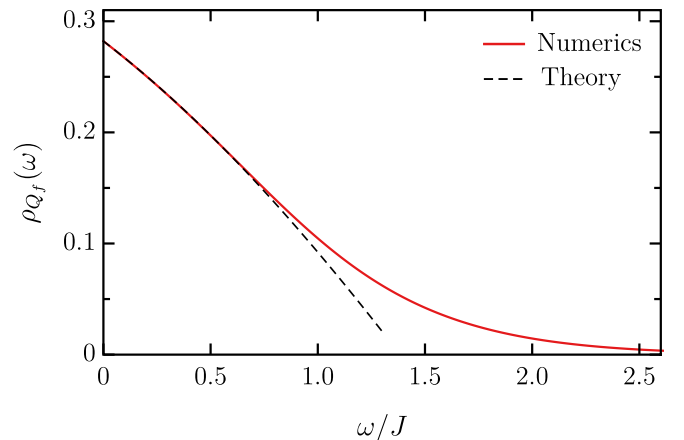
ACKNOWLEDGMENTS

FIG. 14. Plot of the fermionic spin spectral density for $\theta_f = 0$. The red solid line is the numerical result. The black dashed line is the theoretical curve (5.10) plotted for $\alpha_0^A = 0.2643$ and $\alpha_1^A = 0.31$.
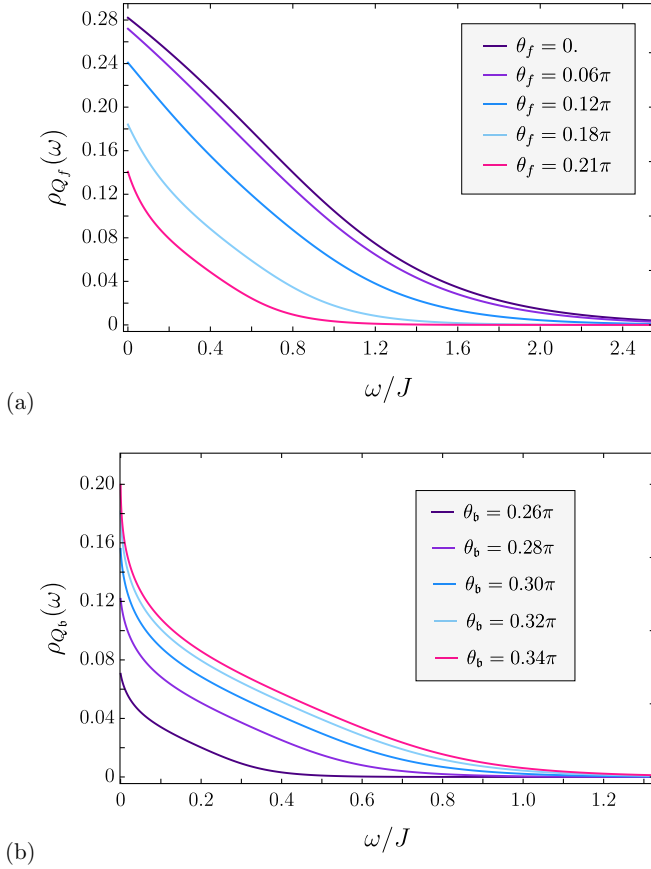
(a)

(b)

FIG. 15. Plots of the numerically computed spin spectral densities (7.12) for (a) fermionic and (b) bosonic spinon models at different values of asymmetry angles.

APPENDIX A: FREE ENERGY FROM CONFORMAL PERTURBATIONS

We can also use the conformal perturbation methods of Sec. III to compute the low-temperature expansion for the free energy. We find [54–56]

$$
\beta F_{\text{SYK}} = \beta F_{\text{CFT}} + \sum_h g_h \int_0^\beta d\tau \langle O_h \rangle_\beta
$$
$$
- \frac{1}{2} \sum_{h,h'} g_h g_{h'} \int_0^\beta d\tau_1 d\tau_2 \langle O_h(\tau_1) O_{h'}(\tau_2) \rangle_\beta
$$

$$
+ \frac{1}{6} \sum_{h,h',h''} g_h g_{h'} g_{h''} \int_0^\beta d\tau_1 d\tau_2 d\tau_2 \langle O_h(\tau_1) O_{h'}(\tau_2)
$$
$$
\times O_{h''}(\tau_3) \rangle_\beta + \cdots . \tag{A1}
$$

The one-point functions in thermal CFT are not necessarily zero and from the scale symmetry we have [57,58]

$$
\langle O_h \rangle_\beta = N b_h / (\beta J)^h. \tag{A2}
$$

To find constants b_h we consider thermal conformal two-point function

$$
G_\beta(\tau) = -\frac{1}{N} \langle \chi_i(\tau) \chi_i(0) \rangle_\beta = -\frac{b^\Delta \text{sgn}(\tau)}{\left| \frac{\beta J}{\pi} \sin \frac{\pi\tau}{\beta} \right|^{2\Delta}}. \tag{A3}
$$

Expanding it in series for $\tau \to 0$ we obtain

$$
G_\beta(\tau) = -\frac{b^\Delta \text{sgn}(\tau)}{|J\tau|^{2\Delta}} \left(1 + \frac{\pi^3}{3} \Delta \left| \frac{\tau}{\beta} \right|^2 \right.
$$
$$
\left. + \frac{\pi^4}{90} \Delta (1 + 5\Delta) \left| \frac{\tau}{\beta} \right|^4 + \cdots \right). \tag{A4}
$$

On the other hand, using the OPE in (3.12), we find

$$
G_\beta(\tau) = -\frac{b^\Delta \text{sgn}(\tau)}{|J\tau|^{2\Delta}} \left(1 + \sum_h c_h |J\tau|^h \langle O_h \rangle_\beta \right), \tag{A5}
$$

where we assumed that the two-point functions of O_h are normalized as in (3.12). Comparing (A4) and (A5), we find that only operators with $h = 2k$, where $k = 1, 2, 3, \ldots$, have a nonzero one-point function, but all operators with $h_1, h_2, h_3, \ldots$ should have zero one-point functions. As we already stressed before, conformal symmetry is broken in the SYK model and the analysis above should be taken with caution. The role of higher expansion terms in (A4) with $k > 1$ is unclear. Moreover, in [28] it was conjectured that the free energy has a term $T^{3.77}$ in the small-T expansion and thus this would imply a nonzero one-point function $\langle O_{h_1} \rangle_\beta$. Whether this is correct or not remains an open question. For the $h_0 = 2$ operator we find $b_0 c_0 = \frac{\pi^2}{3} \Delta$. Thus the contribution of the one-point function of the $h_0 = 2$ operator to the free energy is

$$
\beta \delta F_{h_0} = \beta g_0 \langle O_{h_0} \rangle_\beta = \frac{N \pi^2 \Delta}{3 (\beta J)^2} \frac{\beta g_0}{c_0} = -\frac{2\pi^2 N}{\beta J} \alpha_S, \tag{A6}
$$

where $\alpha_S = \frac{1}{6}(1 - \Delta) b^\Delta |k'_A(2)| \alpha_0$ is the Schwarzian action coupling and this result agrees with [6,7]. For the second-order correction we find

$$
\beta \delta^2 F_h = -\frac{1}{2} \sum_h g_h^2 \int_0^\beta d\tau_1 d\tau_2 \langle O_h(\tau_1) O_h(\tau_2) \rangle = -\frac{1}{2} \sum_h N g_h^2 \beta \int_\epsilon^{\beta-\epsilon} d\tau \left(\frac{\pi}{\beta J \sin \frac{\pi\tau}{\beta}} \right)^{2h}
$$
$$
= -\frac{1}{2} \sum_h \left(\frac{N(g_h^2/J^2)(\beta J)}{(h - 1/2)(\epsilon J)^{2h-1}} + \frac{N(g_h^2/J^2)}{(\beta J)^{2h-2}} \frac{\pi^{2h-1/2} \Gamma\left(\frac{1}{2} - h\right)}{\Gamma(1-h)} \right), \tag{A7}
$$

where we regulated the integral in the UV by a cutoff $\epsilon \sim 1/J$. The first term is proportional to $N(\beta J)$ and represents a correction to the ground energy, whereas the second term is finite and contributes to the free energy of order $1/(\beta J)^{2h-2}$, so we find

$$
\beta \delta^2 F_h = N(q-1) b^\Delta [-k'_A(h)] \frac{(\pi/2)^{2h-1} (\cos \pi h + 1) \Gamma(h)^2}{(2h-1) \cos(\pi h) \Gamma\left(h - \frac{1}{2}\right)^2} \frac{\alpha_h^2}{(\beta J)^{2h-2}}. \tag{A8}
$$

For $h_0 = 2$ this result gives $\beta\delta^2 F_{h_0} = N2\pi^2 q\alpha_S\alpha_0/(\beta J)^2$, which exactly agrees with the $N/(\beta J)^2$ correction computed in [7,28] using careful analysis of the $h_0 = 2$ mode.[4] Moreover, using the result for the large-q free energy from [59], we find, for the $1/(\beta\mathcal{J})^2$ term,

$$\beta F \supset \left(\frac{\pi^2}{q^2} - \frac{\pi^2(24 + 5\pi^2)}{9q^3} + \cdots \right) \frac{N}{(\beta\mathcal{J})^2}. \tag{A9}$$

On the other hand, taking large-q limit of (A8) for the h_0 operator and using that $\tilde\alpha_0 = \frac{2}{q} - \frac{12+7\pi^2}{9q^2} + \cdots$ (see Appendix B), we obtain

$$\beta\delta^2 F_{h_0} = \left(\frac{\pi^2}{q^2} - \frac{\pi^2(24 + 5\pi^2)}{9q^3} + \cdots \right) \frac{N}{(\beta\mathcal{J})^2}. \tag{A10}$$

We see that $\beta\delta^2 F_{h_0}$ exactly coincides with $1/q^2$ and $1/q^3$ orders in the large-q expansion. This implies that if the one-point function $\langle O_{h_1} \rangle_\beta$ is not zero it should start contributing only at the $1/q^4$ order, which seems unlikely. The third-order correction is given by

$$\beta\delta^3 F_{hh'h''} = \frac{1}{6}g_h g_{h'} g_{h''} \int_0^\beta \frac{d\tau_1 d\tau_2 d\tau_3 N c_{hh'h''}}{\left(\frac{\beta J}{\pi}\sin\frac{\pi\tau_{12}}{\beta}\right)^{h+h'-h''}\left(\frac{\beta J}{\pi}\sin\frac{\pi\tau_{13}}{\beta}\right)^{h+h''-h'}\left(\frac{\beta J}{\pi}\sin\frac{\pi\tau_{23}}{\beta}\right)^{h'+h''-h}}$$

$$= \frac{N c_{hh'h''} g_h g_{h'} g_{h''} \Gamma\left(\frac{1-2(h+h'-h'')}{2}\right)\Gamma\left(\frac{1-2(h+h''-h')}{2}\right)\Gamma\left(\frac{1-2(h'+h''-h)}{2}\right)\Gamma\left(1 - h - h' - h''\right)}{6\pi^{\frac{3}{2}-h-h'-h''}(\beta J)^{h+h'+h''}\Gamma(1-2h)\Gamma(1-2h')\Gamma(1-2h'')}. \tag{A11}$$

Using a general expression for $c_{hh'h''}$ [8] for the case when $h = h' = h'' = h_0 \to 2$, we find $c_{h_0 h_0 h_0} \propto 1/(h_0 - 2)^{3/2}$ and therefore the full result (A11) is divergent in this case. This signals that the conformal perturbation theory developed above should be taken very cautiously for the $h_0 = 2$ operator and in general may produce incorrect results.

APPENDIX B: LARGE-q TWO-POINT FUNCTION IN THE FERMIONIC SYK MODEL

We consider the fermionic SYK_q model with zero chemical potential $\mu_f = 0$. In this case there is a particle-hole symmetry and the Schwinger-Dyson equations are $G(i\omega_n)^{-1} = i\omega_n - \Sigma(i\omega_n)$ and $\Sigma(\tau) = J^2 G(\tau)^{q-1}$. At the limit $q \to \infty$ the two-point function at finite temperature $T = 1/\beta$ admits $1/q$ decomposition [6]

$$G(\tau) = -\frac{1}{2}\text{sgn}(\tau)\left(1 + \frac{1}{q}g(\tau) + \frac{1}{q^2}h(\tau) + \cdots\right), \tag{B1}$$

where $g(\tau) = 2\ln\left(\frac{\cos\frac{\pi v}{2}}{\cos x}\right)$ and we defined $x \equiv \frac{\pi v}{2} - \frac{\pi v\tau}{\beta}$, with v found from the transcendental equation $\beta\mathcal{J} = \frac{\pi v}{\cos\frac{\pi v}{2}}$ with rescaled coupling $\mathcal{J} = (2^{1-q}q)^{1/2}J$. The next order $h(\tau)$ was found in [59] and reads

$$h(\tau) = \frac{g^2(x)}{2} - 2\ell(x) - 4\left(\tan x \int_0^x dy\,\ell(y) + 1\right)$$

$$+ \frac{4\left[\tan\frac{\pi v}{2}\int_0^{\pi v/2} dy\,\ell(y) + 1\right](1 + x\tan x)}{1 + \frac{\pi v}{2}\tan\frac{\pi v}{2}}, \tag{B2}$$

where $\ell(x) = g(x) - e^{-g(x)}\text{Li}_2(1 - e^{g(x)})$. Also, the expression for the large-q free energy of the Majorana SYK model is

$$\frac{\beta F}{N} = -\frac{1}{2}\ln 2 - \pi v\left(\tan\frac{\pi v}{2} - \frac{\pi v}{4}\right)\frac{1}{q^2}$$

$$- \pi v\left[\pi v - 2\tan\frac{\pi v}{2}\left(1 - \frac{\pi^2 v^2}{12}\right)\right]\frac{1}{q^3} + \cdots. \tag{B3}$$

At the large-$\beta\mathcal{J}$ limit one finds

$$v = 1 - \frac{2}{\beta\mathcal{J}} + \frac{4}{(\beta\mathcal{J})^2} - \frac{24 + \pi^2}{3(\beta\mathcal{J})^3} + \frac{8(6 + \pi^2)}{3(\beta\mathcal{J})^4} + \cdots. \tag{B4}$$

---

[4]In [6] it was shown that $\langle O_{h_0}(\tau_1)O_{h_0}(\tau_2)\rangle = \frac{N4\pi^2\alpha_S}{\beta^3 J}$ rather than $\langle O_{h_0}(\tau_1)O_{h_0}(\tau_2)\rangle = \frac{N}{|\tau_{12}|^4}$. Nevertheless, in our computation we assumed the latter form of this correlation function and obtained the correct result.

Using this expansion and equations for $g(\tau)$ and $h(\tau)$, we can find at $\beta = \infty$ that $g(\tau) = \ln u^2$ and

$$h(\tau) = -\frac{4}{3}(1-u) - \frac{\pi^2}{9}u(3+u^{-3}) - \frac{2}{3}\ln(u^2) + \frac{1}{6}(4u+3)\ln^2(u^2)$$
$$+ \frac{8}{3}u\ln(u^2)\ln(1+u^{-1}) - \frac{16}{3}u\operatorname{Li}_2(-u^{-1}) + \frac{2}{3}u(2+u^{-3})\operatorname{Li}_2(1-u^2), \tag{B5}$$

where we defined $u \equiv 1/(1+\mathcal{J}\tau)$. The conformal approximation to the two-point function at $\beta = \infty$ has the form

$$G^c(\tau) = -b^{1/q}\frac{\operatorname{sgn}(\tau)}{|\mathcal{J}\tau|^{2/q}}, \quad b = \frac{q-2}{2\pi q}\tan\frac{\pi}{q}. \tag{B6}$$

Therefore, we can write the two-point function (B1) as

$$G(\tau) = G^c(\tau)(\mathcal{J}\tau)^{2/q}\left(\frac{q-2}{\pi}\tan\frac{\pi}{q}\right)^{-1/q}\left(1 + \frac{1}{q}g(\tau) + \frac{1}{q^2}h(\tau) + \cdots\right)$$
$$= G^c(\tau)\left(1 + \frac{2\ln\mathcal{J}\tau}{q} + \frac{2(1+\ln^2\mathcal{J}\tau)}{q^2} + \cdots\right)\left(1 - \frac{2\ln(1+\mathcal{J}\tau)}{q} + \frac{1}{q^2}h(\tau) + \cdots\right). \tag{B7}$$

Finally, using the result (B5) and expanding everything in the limit $\mathcal{J}\tau \to \infty$, we find

$$G(\tau) = G^c(\tau)\left\{1 + \left(-\frac{2}{\mathcal{J}\tau} + \frac{1}{(\mathcal{J}\tau)^2} - \frac{2}{3(\mathcal{J}\tau)^3} + \cdots\right)\frac{1}{q} + \left[\frac{12+7\pi^2}{9}\left(\frac{1}{\mathcal{J}\tau} - \frac{1}{(\mathcal{J}\tau)^2} + \frac{1}{(\mathcal{J}\tau)^3}\right)\right.\right.$$
$$\left.\left. - \frac{7}{2(\mathcal{J}\tau)^2} + \frac{3}{(\mathcal{J}\tau)^3} - \frac{6\ln(\mathcal{J}\tau)}{(\mathcal{J}\tau)^2} + \frac{12\ln(\mathcal{J}\tau)}{(\mathcal{J}\tau)^3} + \cdots\right]\frac{1}{q^2} + \cdots\right\}. \tag{B8}$$

On the other hand, from the resonance theory described in Sec. IV we expect to have

$$G(\tau) = G^c(\tau)\left(1 - \sum_{k=0}^{\infty}\frac{\alpha_k}{|\mathcal{J}\tau|^{h_k-1}} - \sum_{k,m=0}^{\infty}\frac{a_{km}\alpha_k\alpha_m}{|\mathcal{J}\tau|^{h_k+h_m-2}} - \sum_{k,m,l=0}^{\infty}\frac{a_{kml}\alpha_k\alpha_m\alpha_l}{|\mathcal{J}\tau|^{h_k+h_m+h_l-3}} - \cdots\right), \tag{B9}$$

where α_k, a_{km}, and a_{kml} are all functions of q. In the large-q limit solving $k_A(h) = 1$, where

$$k_A(h) = \frac{\Gamma(2\Delta - h)\Gamma(2\Delta + h - 1)}{\Gamma(2\Delta - 2)\Gamma(2\Delta + 1)}\left(1 - \frac{\sin(\pi h)}{\sin(2\pi\Delta)}\right), \tag{B10}$$

we find that operator dimensions apart from $h_0 = 2$ admit $1/q$ decomposition and read

$$h_1 = 3 + \frac{4}{q} + \cdots, \quad h_2 = 5 + \frac{22}{9q} + \cdots, \quad h_k = 2k + 1 + \frac{2(2k^2+k+1)}{(k+1)(2k-1)q} + \cdots. \tag{B11}$$

Using these anomalous dimensions in (B9), we find

$$G(\tau) = G^c(\tau)\left(1 - \frac{\tilde{\alpha}_0}{(\mathcal{J}\tau)} - \frac{a_{00}\tilde{\alpha}_0^2}{(\mathcal{J}\tau)^2} - \frac{\tilde{\alpha}_1}{(\mathcal{J}\tau)^{2+4/q+\cdots}} - \frac{a_{000}\tilde{\alpha}_0^3}{(\mathcal{J}\tau)^3} - \frac{2a_{01}\tilde{\alpha}_0\tilde{\alpha}_1}{(\mathcal{J}\tau)^{3+4/q+\cdots}} - \frac{\tilde{\alpha}_2}{(\mathcal{J}\tau)^{4+22/9q+\cdots}} - \cdots\right)$$
$$= G^c(\tau)\left[1 - \frac{\tilde{\alpha}_{h_0}}{(\mathcal{J}\tau)} - \frac{a_{00}\tilde{\alpha}_0^2}{(\mathcal{J}\tau)^2} - \frac{\tilde{\alpha}_1}{(\mathcal{J}\tau)^2}\left(1 - \frac{4}{q}\ln(\mathcal{J}\tau) + \cdots\right)\right.$$
$$\left. - \frac{\tilde{\alpha}_2}{(\mathcal{J}\tau)^4}\left(1 - \frac{22}{9q}\ln(\mathcal{J}\tau) + \cdots\right) - \cdots\right], \tag{B12}$$

where we defined $\tilde{\alpha}_k(q) = (2^{1-q}q)^{(h_k-1)/2}\alpha_k(q)$. Comparing (B8) and (B12), we find the relations

$$\tilde{\alpha}_0(q) = \frac{2}{q} - \frac{12+7\pi^2}{9q^2} + \cdots, \quad \tilde{\alpha}_1(q) = -\frac{3}{2q} + \frac{7\pi^2 + 33 - 24a_{00}^{(2)}}{6q^2} + \cdots, \quad a_{00}(q) = \frac{q}{8} + a_{00}^{(2)} + \cdots,$$
$$a_{01}(q) = -\frac{q}{2} + a_{01}^{(2)} + \cdots, \quad a_{000}(q) = -\frac{7}{24}q^2 + \frac{1}{8}\left(6a_{01}^{(2)} - 8a_{00}^{(2)} + 4\right)q + \cdots. \tag{B13}$$

We note that the $\ln(\mathcal{J}\tau)/(\mathcal{J}\tau)^2$ and $\ln(\mathcal{J}\tau)/(\mathcal{J}\tau)^3$ terms in $1/q^2$ order arise due to the h_1 operator. The large-q results (B13) for a_{00}, a_{01}, and a_{000} match with arbitrary q formulas (4.43) and (4.48) derived in Sec. IV. This comparison also sets $a_{00}^{(2)} = 0$ and $a_{01}^{(2)} = -3/2$.

APPENDIX C: TWO-POINT FUNCTION FOR $q = 2$ IN THE FERMIONIC SYK MODEL

For $q = 2$ the exact result for the two-point function for $\tau > 0$ at zero temperature is [6]

$$G(\tau) = -\int_0^\pi \frac{d\theta}{\pi} \cos^2 \theta e^{-2J\tau \sin\theta} = \frac{L_1(2J\tau) - I_1(2J\tau)}{2J\tau} = -\frac{1}{\pi J\tau} + \frac{1}{4\pi(J\tau)^3} + \frac{3}{16\pi(J\tau)^5} + \cdots, \qquad \text{(C1)}$$

where $I_1(x)$ and $L_1(x)$ are modified Bessel and Struve functions. For $q = 2$ the conformal two-point function is

$$G^c(\tau) = -\frac{1}{\pi J\tau}, \qquad \text{(C2)}$$

where we used that $b^{1/2} = 1/\pi$. Thus we find

$$G(\tau) = G^c(\tau)\left(1 - \frac{1}{4(J\tau)^2} - \frac{3}{16(J\tau)^4} - \frac{45}{64(J\tau)^6} - \cdots\right). \qquad \text{(C3)}$$

On the other hand, using the formula (B9) and that for $q = 2$ operators dimensions are simply $h_k = 2(k + 1)$, we expect to have

$$G(\tau) = G^c(\tau)\left(1 - \sum_{k=0}^\infty \frac{\alpha_k}{(J\tau)^{2k+1}} - \sum_{k,m=0}^\infty \frac{a_{km}\alpha_k\alpha_m}{(J\tau)^{2(k+m+1)}} - \sum_{k,m,l=0}^\infty \frac{a_{kml}\alpha_k\alpha_m\alpha_l}{(J\tau)^{2(k+m+l)+3}} - \cdots\right). \qquad \text{(C4)}$$

Comparing (C3) and (C4), we obtain relations between $\alpha_k(q)$ and $a_{km}(q)$, $a_{kml}(q)$, etc., for $q = 2$,

$$\alpha_0(2) = 0, \quad \alpha_1(2) = -a_{000}(2)\alpha_0^3(2),$$
$$a_{00}(2)\alpha_0^2(2) = \tfrac{1}{4}, \quad 2a_{01}(2)\alpha_0(2)\alpha_1(2) = \tfrac{3}{16}. \qquad \text{(C5)}$$

Moreover, using that $\alpha_0(q) = \frac{\pi}{8}(q - 2) + \cdots$ for $q \to 2$ [6], we obtain that $a_{00}(q) \to \frac{16}{\pi^2(q-2)^2} + \cdots$, which agrees with the arbitrary q formula (4.43) for $a_{hh'}(q)$.

APPENDIX D: FINITE-TEMPERATURE GENERALIZATION FOR SPECTRAL DENSITIES

Consider the retarded Green's function in real time

$$G_{fR}(t) = -i\theta(t)\langle\{f(t), f^\dagger(0)\}\rangle,$$
$$G_{\mathfrak{b}R}(t) = -i\theta(t)\langle[\mathfrak{b}(t), \mathfrak{b}^\dagger(0)]\rangle, \qquad \text{(D1)}$$

where $\Theta(t)$ is the Heaviside step function and should not be confused with the asymmetry angle. Below we again suppress subscript $a = f, \mathfrak{b}$ and only retain the ζ factor, where $\zeta_f = -1$ and $\zeta_\mathfrak{b} = 1$. We can obtain the retarded Green's function by analytically continuing the imaginary-time one:

$$G_R(t) = i\theta(t)[G(it + 0) - G(it - 0)]. \qquad \text{(D2)}$$

The full retarded Green's function can be written as a conformal part plus corrections $G_R(t) = G_R^c(t) + \delta G_R(t)$ and for the conformal retarded Green's function we find

$$G_R^c(t) = -i\theta(t)\frac{(e^{-i\pi(\Delta+i\mathcal{E})} - \zeta e^{i\pi(\Delta+i\mathcal{E})})b^\Delta e^{-(2\pi/i\mathcal{E}\beta)t}}{\left(\frac{\beta J}{\pi}\sinh\frac{\pi t}{\beta}\right)^{2\Delta}}. \qquad \text{(D3)}$$

We split the correction $\delta G_R(t)$ into two terms $\delta G_R(t) = \delta G_R^A(t) + \delta G_R^S(t)$, where

$$\delta_h G_R^{A/S}(t) = -\frac{1}{2}(v_{h+} \pm v_{h-})\frac{\alpha_h}{(\beta J)^{h-1}}f_{Rh}^{A/S}(t)G_R^c(t), \quad \text{(D4)}$$

and for $f_{Rh}^{A/S}(t)$ we have

$$f_{Rh}^{A/S}(t) = \frac{e^{-i\pi(\Delta+i\mathcal{E})}f_h^{A/S}(it+0) \mp \zeta e^{i\pi(\Delta+i\mathcal{E})}f_h^{A/S}(it-0)}{e^{-i\pi(\Delta+i\mathcal{E})} - \zeta e^{i\pi(\Delta+i\mathcal{E})}}, \qquad \text{(D5)}$$

where the functions $f_h^{A/S}(\tau)$ are defined in (4.56) and (4.57). To find $f_h^{A/S}(it \pm 0)$ we note that function $A_h(u)$ is analytic in $\mathbf{C}$ and has a branch cut $[1, +\infty)$. Inside the unit circle $|u| \leqslant 1$ we can compute $A_h(u)$ using a series expansion. Analytic continuation of $f_h^{A/S}(\tau)$ will produce two terms $A_h(e^{-2\pi/t\beta})$ and $A_h(e^{2\pi/t\beta} \pm i0)$, where the last function is computed above or below the branch cut. Using formulas for linear transformations of the hypergeometric function, we can represent $f_h^A(it \pm 0)$ in the convenient form

$$f_h^A(it \pm 0) = \frac{\pi(2\pi)^{h-1}\Gamma(h)^2}{2\sin\frac{\pi h}{2}\sin(2\pi h)\Gamma(2h-1)}\left(\frac{(1 + e^{\pm i\pi h})B_h(e^{-2\pi t/\beta})}{\Gamma(1-h)^2} - (h \to 1-h)\right),$$

$$f_h^S(it \pm 0) = \pm\frac{i\pi(2\pi)^{h-1}\Gamma(h)^2}{2\cos\frac{\pi h}{2}\sin(2\pi h)\Gamma(2h-1)}\left(\frac{(1 - e^{\pm i\pi h})B_h(e^{-2\pi t/\beta})}{\Gamma(1-h)^2} - (h \to 1-h)\right), \qquad \text{(D6)}$$

where $B_h(u) = (1 - u)^h \mathbf{F}(h, h, 2h, 1 - u)$ is unambiguous for $u = e^{-2\pi t/\beta}$ and can be computed using series expansion. We note that B_h coincides with the function $B_{h,0}^+$ used in [7,22,36]. Using (D5), we obtain, for the fermions,

$$f_{Rh}^A(t) = \frac{(2\pi)^{h-2}\cos\frac{\pi h}{2}\Gamma(h)^2}{\cos(\pi h)\Gamma(2h-1)}\left[\Gamma(h)^2\left(1 + \frac{\cos\pi(\Delta - h + i\mathcal{E})}{\cos\pi(\Delta + i\mathcal{E})}\right)B_h(e^{-2\pi t/\beta}) - (h \to 1 - h)\right],$$

$$f_{Rh}^S(t) = \frac{i(2\pi)^{h-2}\sin\frac{\pi h}{2}\Gamma(h)^2}{\cos(\pi h)\Gamma(2h-1)}\left[\Gamma(h)^2\left(1 - \frac{\cos\pi(\Delta - h + i\mathcal{E})}{\cos\pi(\Delta + i\mathcal{E})}\right)B_h(e^{-2\pi t/\beta}) - (h \to 1 - h)\right], \tag{D7}$$

and for bosons we need to change $\cos \to \sin$ inside the brackets. For the $h_0^A = 2$ mode we find

$$f_{R0}^A(t) = 2 - \frac{\pi\tan[\pi(\Delta + i\mathcal{E})] + \frac{2\pi t}{\beta}}{\tanh\frac{\pi t}{\beta}}, \quad f_{R0}^S(t) = -\frac{i\pi}{\tanh\frac{\pi t}{\beta}} \tag{D8}$$

and for bosons we need to change $\tan \to -\cot$. To compute the expression for the spectral density we need to find the retarded Green's function in frequency space $G_R(\omega) = G_R^c(\omega) + \delta G_R(\omega)$. For the conformal part we take the Fourier transform of (D3) and find

$$G_R^c(\omega) = -i\frac{C}{J}\left(\frac{\beta J}{2\pi}\right)^{1-2\Delta}e^{-i\theta}\frac{\Gamma(\Delta - i\omega')}{\Gamma(1 - \Delta - i\omega')}, \tag{D9}$$

where $\omega' \equiv \frac{\beta\omega}{2\pi} - \mathcal{E}$ and the constant C is defined after (4.16). Formulas written with the use of the asymmetry angle are the same for both fermions and bosons. Next, for $\delta G_R(\omega) = \delta G_R^A(\omega) + \delta G_R^S(\omega)$ we introduce $f_{Rh}^{A/S}(\omega)$ as

$$\delta_h G_R^{A/S}(\omega) = -\frac{1}{2}(v_{h+} \pm v_{h-})\frac{\alpha_h}{(\beta J)^{h-1}}f_{Rh}^{A/S}(\omega)G_R^c(\omega). \tag{D10}$$

We stress that $f_{Rh}^{A/S}(\omega)$ are not Fourier transforms just of $f_{Rh}^{A/S}(t)$. After some computations we obtain

$$f_{Rh}^A(\omega) = \frac{(2\pi)^{h-2}\cos\frac{\pi h}{2}\Gamma(h)^2}{\cos(\pi h)\Gamma(2h-1)}\left[\frac{\Gamma(h)}{\Gamma(1-h)}\left(e^{2i\theta} - \frac{\sin\left(\frac{\pi h}{2} - 2\pi\Delta\right)}{\sin\frac{\pi h}{2}}\right)J_h(\omega) - (h \to 1 - h)\right],$$

$$f_{Rh}^S(\omega) = \frac{i(2\pi)^{h-2}\sin\frac{\pi h}{2}\Gamma(h)^2}{\cos(\pi h)\Gamma(2h-1)}\left[\frac{\Gamma(h)}{\Gamma(1-h)}\left(\frac{\cos\left(\frac{\pi h}{2} - 2\pi\Delta\right)}{\cos\frac{\pi h}{2}} - e^{2i\theta}\right)J_h(\omega) - (h \to 1 - h)\right], \tag{D11}$$

where the function $J_h(\omega)$ is

$$J_h(\omega) = \Gamma(1 - \Delta - i\omega')\Gamma(1 + h - 2\Delta)\Gamma(2\Delta)\,_3\mathbf{F}_2\begin{pmatrix} h & h & 1 + h - 2\Delta \\ 2h & 1 + h - \Delta - i\omega' \end{pmatrix}; 1\end{pmatrix} \tag{D12}$$

and $_3\mathbf{F}_2$ is the regularized hypergeometric function. For $h_0^A = 2$ we find $f_{R0}^S(\omega) = \pi\omega'/\Delta$ and

$$f_{R0}^A(\omega) = \frac{1}{\Delta}(2\Delta - 1 - i\omega'\{\pi\tan[\pi(\Delta + i\mathcal{E})] + \psi(1 - \Delta - i\omega') - \psi(\Delta - i\omega')\}), \tag{D13}$$

where $\psi(z) \equiv \Gamma'(z)/\Gamma(z)$ is the digamma function and we used that $\tan\pi(\Delta + i\mathcal{E}) = \tan\pi\Delta + (e^{2i\theta} - 1)/\sin 2\pi\Delta$ for fermions. For bosons we need to change $\tan \to -\cot$.

For the spectral density we find $\rho(\omega) = \rho^c(\omega) + \delta\rho(\omega)$, where

$$\rho^c(\omega) = -\frac{1}{\pi}\text{Im}G_R^c(\omega) = \frac{C}{\pi J}\left(\frac{\beta J}{2\pi}\right)^{1-2\Delta}\text{Re}\left(e^{-i\theta}\frac{\Gamma(\Delta - i\omega')}{\Gamma(1 - \Delta - i\omega')}\right) \tag{D14}$$

and the correction is

$$\delta\rho(\omega) = \sum_h \frac{\alpha_h}{2\pi(\beta J)^{h-1}}\left\{(v_{h+} + v_{h-})\text{Im}\left[G_R^c(\omega)f_{Rh}^A(\omega)\right] + (v_{h+} - v_{h-})\text{Im}\left[G_R^c(\omega)f_{Rh}^S(\omega)\right]\right\}. \tag{D15}$$

Finally, we find formulas for the spin-spin correlator and spin-spin spectral density at nonzero temperature. The spin-spin correlator in imaginary time is $Q(\tau) = -\zeta G(\tau)G(-\tau)$ [note that $Q(\tau)$ is denoted by $\chi_L(\tau)$ in Sec. I]. Retaining only leading linear corrections, we obtain

$$Q(\tau) = Q^c(\tau)\left(1 - \sum_h (v_{h+} + v_{h-})\frac{\alpha_h}{(\beta J)^{h-1}}f_h^A(\tau) - \cdots\right), \tag{D16}$$

where we note that the functions $f_h^S(\tau)$ do not contribute at the leading order and the conformal part of the spin-spin correlator is

$$Q^c(\tau) = -\zeta G^c(\tau)G^c(-\tau) = -\frac{b^{2\Delta}}{\left|\frac{\beta J}{\pi}\sin\frac{\pi\tau}{\beta}\right|^{4\Delta}}. \quad (D17)$$

We can find the retarded spin-spin correlator in real time $Q_R(t) = -i\theta(t)\langle[S(t), S(0)]\rangle$ by analytic continuation of the imaginary-time one:

$$Q_R(t) = i\theta(t)[Q(it + 0) - Q(it - 0)]. \quad (D18)$$

We note that all formulas for $Q_R(t)$ are essentially the same as for bosonic $G_R(t)$ with the replacement $\Delta \to 2\Delta$ and $\mathcal{E} = 0$ (or $\theta = \pi/2$). Below we still repeat some main steps.

As usual, $Q_R(t)$ is split into two terms $Q_R(t) = Q_R^c(t) + \delta Q_R(t)$, where the conformal part and correction have the

forms

$$Q_R^c(t) = -\theta(t)\frac{2\sin(2\pi\Delta)b^{2\Delta}}{\left(\frac{\beta J}{\pi}\sinh\frac{\pi t}{\beta}\right)^{4\Delta}}, \quad (D19)$$

$$\delta_h Q_R(t) = -(v_{h+} + v_{h-})\frac{\alpha_h}{(\beta J)^{h-1}}f_{Rh}^A(t)Q_R^c(t).$$

Here the bosonic function $f_{Rh}^A(t)$ in (D7) is for $\mathcal{E} = 0$ and $\Delta \to 2\Delta$. Now taking the Fourier transform of $Q_R(t)$, we get $Q_R(\omega) = Q_R^c(\omega) + \delta Q_R(\omega)$, where the conformal part is

$$Q_R^c(\omega) = -\frac{\pi b^{2\Delta}}{J\Gamma(4\Delta)\cos 2\pi\Delta}\left(\frac{\beta J}{2\pi}\right)^{1-4\Delta}\frac{\Gamma\left(2\Delta - i\frac{\beta\omega}{2\pi}\right)}{\Gamma\left(1 - 2\Delta - i\frac{\beta\omega}{2\pi}\right)}. \quad (D20)$$

The correction has the form

$$\delta Q_R(\omega) = -\sum_h(v_{h+} + v_{h-})\frac{\alpha_h}{(\beta J)^{h-1}}f_{Rh}^A(\omega)Q_R^c(\omega), \quad (D21)$$

where the function $f_{Rh}^A(\omega)$ in (D11) is computed here for $\Delta \to 2\Delta$, $\theta = \pi/2$, and $\omega' = \frac{\beta\omega}{2\pi}$. Therefore, for the $h_0^A = 2$ mode we find

$$f_{R0}^A(\omega) = \frac{1}{2\Delta}\left\{4\Delta - 1 - i\frac{\beta\omega}{2\pi}\left[\psi\left(1 - 2\Delta - i\frac{\beta\omega}{2\pi}\right) - \psi\left(2\Delta - i\frac{\beta\omega}{2\pi}\right) - \pi\cot 2\pi\Delta\right]\right\}. \quad (D22)$$

We are mainly interested in the $\Delta = 1/4$ case. At the $\Delta \to 1/4$ limit the conformal part $Q_R^c(\omega)$ is diverging and we get

$$Q_R^c(\omega) = \frac{2b^{1/2}}{J}\left[\frac{1}{4\left(\Delta - \frac{1}{4}\right)} + \psi\left(\frac{1}{2} - \frac{i\beta\omega}{2\pi}\right) + \gamma - \ln\left(\frac{\beta J}{2\pi}\right) + \cdots\right]. \quad (D23)$$

The diverging part is real and does not contribute to the spectral density. On the other hand, the function $f_{Rh}^A(\omega)$ goes to zero as $\Delta - 1/4$ and we obtain

$$f_{Rh}^A(\omega)Q_R^c(\omega) = -\frac{b^{1/2}(2\pi)^{h-1}\cos\frac{\pi h}{2}\Gamma(h)^2}{J\cos(\pi h)\Gamma(2h-1)}\left[\frac{\Gamma(h)^2\Gamma\left(\frac{\pi - i\beta\omega}{2\pi}\right)}{\tan\frac{\pi h}{2}\Gamma(1-h)}\,_3\mathbf{F}_2\left(\begin{array}{c}h\ h\ h\\2h\ \frac{\pi(2h+1)-i\beta\omega}{2\pi}\end{array};1\right) - (h \to 1 - h)\right], \quad (D24)$$

where $_3\mathbf{F}_2$ is the regularized hypergeometric function. The spin-spin spectral density $\rho_Q(\omega)$ can be found as

$$\rho_Q(\omega) = -\frac{1}{\pi}\text{Im}Q_R(\omega). \quad (D25)$$

We write $\rho_Q(\omega) = \rho_Q^c(\omega) + \delta\rho_Q(\omega)$ and using (D24) we obtain

$$\rho_Q(\omega) = \frac{b^{1/2}}{J}\tanh\left(\frac{\beta\omega}{2}\right)\left[1 - \sum_h(v_{h+} + v_{h-})\frac{\alpha_h}{(\beta J)^{h-1}}\mathcal{R}_h^A\left(\frac{\beta\omega}{2\pi}\right) - \cdots\right], \quad (D26)$$

where the function $\mathcal{R}_h^A(\omega)$ is

$$\mathcal{R}_h^A(\omega) = \frac{2\left(\frac{\pi}{2}\right)^h\Gamma(h)}{\sqrt{\pi}\sin\left(\frac{\pi h}{2}\right)\Gamma\left(h - \frac{1}{2}\right)}\text{Re}\,_3\mathbf{F}_2\left(\begin{array}{c}h\ 1 - h\ \frac{1}{2} + i\omega\\1\ 1\end{array};1\right). \quad (D27)$$

To get this expression we used two identities for the regularized hypergeometric function

$$_3\mathbf{F}_2\left(\begin{array}{c}1 - h\ 1 - h\ 1 - h\\2 - 2h\ 1 - h + a\end{array};1\right) = \frac{\Gamma(h)^3}{\Gamma(1-h)^3}\,_3\mathbf{F}_2\left(\begin{array}{c}h\ h\ h\\2h\ h + a\end{array};1\right) + \frac{\Gamma(h)^3}{\Gamma(a)\Gamma(2-2h)\Gamma(2h-1)}\,_3\mathbf{F}_2\left(\begin{array}{c}1 - h\ h\ 1 - a\\1\ 1\end{array};1\right), \quad (D28)$$

$$_3\mathbf{F}_2\left(\begin{array}{c}h\ h\ h\\2h\ h + a\end{array};1\right) = \frac{\Gamma(1-a)\Gamma(1-h)^2}{\Gamma(h)\Gamma(h+a)\Gamma(1-h-a)}\,_3\mathbf{F}_2\left(\begin{array}{c}h\ 1 - h\ 1 - a\\1\ 1\end{array};1\right) + \frac{\Gamma(1-h)^2}{\Gamma(h)\Gamma(a)}\,_3\mathbf{F}_2\left(\begin{array}{c}h\ 1 - h\ a\\1\ 1\end{array};1\right). \quad (D29)$$

Retaining only the $h_0^A = 2$ mode, we obtain

$$\rho_Q(\omega) = \frac{b^{1/2}}{J}\tanh\left(\frac{\beta\omega}{2}\right)\left[1 - \frac{2\alpha_0^A\omega}{J}\tanh\left(\frac{\beta\omega}{2}\right) - \cdots\right], \quad (D30)$$

where we used that $v_{0+} + v_{0-} = 2$ and

$$_3\mathbf{F}_2\left(\begin{matrix} 1-h & h & \frac{1}{2}+i\omega \\ & 1 & 1 \end{matrix}; 1\right) = -2i\omega - 2i\omega\left[\psi\left(\tfrac{1}{2}-i\omega\right) + \gamma_E\right](h-2) + O((h-2)^2). \tag{D31}$$

APPENDIX E: ZERO-TEMPERATURE NUMERICS FOR THE BOSONIC/FERMIONIC SYK AND RANDOM ROTOR MODELS

We consider Dyson-Schwinger equations for the retarded Green's function for bosonic and fermionic SYK models for the $q = 4$ case, which is obtained by analytic continuation from the Matsubara frequency $i\omega_n \to \omega + i0$. The first Dyson-Schwinger equation reads

$$G_R(\omega)^{-1} = \omega + i0 + \mu - \Sigma_R(\omega). \tag{E1}$$

Here, for brevity, we do not explicitly label Green's functions by the index $a = f, \mathfrak{b}$ but we will use the symbol ζ_a, which is $\zeta_f = -1$ and $\zeta_\mathfrak{b} = 1$. In general, for the Green's function and self-energy we define analytically the upper half-plane functions $G(z)$ and $\Sigma(z)$, which are expressed through the spectral densities $\rho(\omega)$ and $\sigma(\omega)$ as

$$G(z) = \int_{-\infty}^{+\infty} d\omega \frac{\rho(\omega)}{z-\omega}, \quad \Sigma(z) = \int_{-\infty}^{+\infty} d\omega \frac{\sigma(\omega)}{z-\omega}. \tag{E2}$$

The Matsubara and retarded Green's functions can be obtained from these functions by taking $z = i\omega_n$ and $z = \omega + i0$. We can find the spectral density as $\rho(\omega) = -\frac{1}{\pi}\mathrm{Im}G_R(\omega)$. Also, using the representation (E2), we can obtain the Green's function in imaginary time expressed through the integral over the spectral density

$$\begin{aligned} G(\tau) &= \frac{1}{\beta} \sum_n G(i\omega_n) e^{-i\omega_n \tau} \\ &= -\int_{-\infty}^{+\infty} d\omega \frac{\rho(\omega) e^{-\omega\tau}}{1 - \zeta e^{-\beta\omega}}, \quad \tau \in (0, \beta). \end{aligned} \tag{E3}$$

We note that $\zeta G(\beta^-) - G(0^+) = \int_{-\infty}^{+\infty} d\omega\, \rho(\omega) = 1$ for arbitrary temperature. To obtain the second Dyson-Schwinger equation for the retarded self-energy $\Sigma_R(\omega)$ we consider this equation in the Matsubara space $\Sigma(\tau) = J^2 G^2(\tau) G(\beta - \tau)$ and use (E3) to write it through the spectral density

$$\Sigma(i\omega_n) = -J^2 \int_{-\infty}^{+\infty} \prod_{i=1}^{3} [d\omega_i \rho(\omega_i)] \frac{n(\omega_1)n(\omega_2)n(-\omega_3) + n(-\omega_1)n(-\omega_2)n(\omega_3)}{\omega_1 + \omega_2 - \omega_3 - i\omega_n}, \tag{E4}$$

where $n(\omega) = 1/(e^{\beta\omega} - \zeta)$ is the Bose or Fermi distribution and we can get $\Sigma_R(\omega) = \Sigma(i\omega_n = \omega + i0)$. At zero temperature $\beta = \infty$ we can replace $n_\mathfrak{b}(\omega)$ by $-\theta(-\omega)$ and $n_f(\omega)$ by $\theta(-\omega)$. Though $n_\mathfrak{b}(\omega)$ is divergent for $\omega \to 0$, we assume that this divergence does not play any role. The functions $G_R(\omega)$ and $\Sigma_R(\omega)$ are complex valued and further we will adopt notation for their real and imaginary parts $G_R(\omega) = G'(\omega) + iG''(\omega)$ and $\Sigma_R(\omega) = \Sigma'(\omega) + i\Sigma''(\omega)$. So for $\beta = \infty$, using (E4), we find

$$\Sigma''(\omega) = \begin{cases} \zeta\pi J^2 \int_0^{\omega_1+\omega_2\leqslant\omega} d\omega_1 d\omega_2 \rho(\omega_1)\rho(\omega_2)\rho(\omega_1+\omega_2-\omega), & \omega > 0 \\ \zeta\pi J^2 \int_{\omega_1+\omega_2\geqslant\omega}^0 d\omega_1 d\omega_2 \rho(\omega_1)\rho(\omega_2)\rho(\omega_1+\omega_2-\omega), & \omega < 0. \end{cases} \tag{E5}$$

Below in all formulas we set $J = 1$ for brevity. We anticipate that at zero temperature the functions $\rho(\omega)$ and $\Sigma''(\omega)$ will have discontinuity. So it will be convenient to use a new set of functions defined separately for $\omega > 0$ and $\omega < 0$,

$$\rho(\omega) = \begin{cases} \frac{g_+(\omega)}{\sqrt{\omega}}, & \omega > 0 \\ \frac{g_-(-\omega)}{\sqrt{-\omega}}, & \omega < 0, \end{cases}$$

$$\Sigma''(\omega) = \begin{cases} 4\pi\sqrt{\omega}s_+(\omega), & \omega > 0 \\ 4\pi\sqrt{-\omega}s_-(-\omega), & \omega < 0. \end{cases} \tag{E6}$$

We make the change of variables $\omega_1 = \omega \sin^2 u \cos^2 \phi$ and $\omega_2 = \omega \sin^2 u \sin^2 \phi$ in (E5) and obtain

$$s_\pm(\omega) = \zeta \int_0^{\pi/2} du \sin u \int_0^{\pi/2} d\phi\, g_\pm(\omega \sin^2 u \cos^2 \phi) g_\pm(\omega \sin^2 u \sin^2 \phi) g_\mp(\omega \cos^2 u). \tag{E7}$$

We note that $s_\pm(x)$ and $g_\pm(x)$ are defined only for a positive argument. Now it is left to find a real part $\Sigma'(\omega)$ of the self-energy. For this we use the Kramers-Kronig relation

$$\Sigma'(\omega) = \fint_{-\infty}^{+\infty} \frac{d\nu}{\pi} \frac{\Sigma''(\nu) - \Sigma''(\omega)}{\nu - \omega}. \tag{E8}$$

Defining $\Sigma'_\pm(\omega)$ as $\Sigma'(\omega) = \Sigma'_+(\omega)\theta(\omega) + \Sigma'_-(-\omega)\theta(-\omega)$, we find

$$\Sigma'_\pm(\omega) = \pm\fint_0^{+\infty} \frac{d\nu}{\pi} \left(\frac{\Sigma''_\pm(\nu) - \Sigma''_\pm(\omega)}{\nu - \omega} - \frac{\Sigma''_\mp(\nu) - \Sigma''_\pm(\omega)}{\nu + \omega} \right). \tag{E9}$$

At zero temperature we set the chemical potential $\mu = \Sigma'(\omega = 0)$, so introducing $h_\pm(\omega)$ as

$$\Sigma'(\omega) - \Sigma'(0) = \begin{cases} 4\sqrt{\omega}h_+(\omega), & \omega > 0 \\ 4\sqrt{-\omega}h_-(-\omega), & \omega < 0 \end{cases} \tag{E10}$$

and simplifying expressions, we finally obtain

$$h_\pm(\omega) = \pm \fint_0^{+\infty} dv \left(\frac{\sqrt{\omega}s_\pm(v) - \sqrt{v}s_\pm(\omega)}{\sqrt{v}(v - \omega)} + \frac{\sqrt{\omega}s_\mp(v) + \sqrt{v}s_\pm(\omega)}{\sqrt{v}(v + \omega)} \right). \tag{E11}$$

Now using the first Dyson-Schwinger equation, we can get $g_\pm$ from $s_\pm$ and $h_\pm$,

$$g_\pm(\omega) = -\frac{4s_\pm(\omega)}{[4h_\pm(\omega) \mp \sqrt{\omega}]^2 + 16\pi^2[s_\pm(\omega)]^2}. \tag{E12}$$

We solve Dyson-Schwinger equations iteratively using (E7), (E11), and (E12) and also imposing the initial conditions coming from the conformal solution (4.16),

$$g_\pm(0) = \frac{C \sin\left(\frac{\pi}{4} \pm \theta\right)}{\pi}, \quad s_\pm(0) = -\frac{\sin\left(\frac{\pi}{4} \pm \theta\right)}{4\pi C},$$

$$h_\pm(0) = \mp\frac{\cos\left(\frac{\pi}{4} \pm \theta\right)}{4C}, \quad C = \left(\frac{-\zeta\pi}{\cos 2\theta}\right)^{1/4}. \tag{E13}$$

We can compute the chemical potential numerically using that $\mu = \Sigma'(\omega = 0)$ and Eq. (E9):

$$\mu = 4 \int_0^{+\infty} d\omega \frac{s_+(\omega) - s_-(\omega)}{\sqrt{\omega}}. \tag{E14}$$

In the random rotor model defined in Sec. VI the spectral density $\rho(\omega)$ is an odd function due to the particle-hole symmetry. Thus we have $g_-(\omega) = -g_+(\omega)$ and $s_-(\omega) = -s_+(\omega)$, where the equation for $s_+(\omega)$ is written in (E7) ($\zeta = 1$ in this case). Also, $h_-(\omega) = h_+(\omega)$ and from (E11) we find

$$h_+(\omega) = \int_0^{+\infty} dv \frac{2\omega[\sqrt{\omega}s_+(v) - \sqrt{v}s_+(\omega)]}{\sqrt{v}(v^2 - \omega^2)}. \tag{E15}$$

The first Schwinger-Dyson equation in the random rotor model reads

$$g_+(\omega) = -\frac{4s_+(\omega)}{[\omega^{3/2} - 4h_+(\omega)]^2 + 16\pi^2 s_+(\omega)^2} \tag{E16}$$

and the boundary conditions are obtained from (E13) for $\theta = \pi/2$.

[1] S. Sachdev and J. Ye, Gapless Spin-Fluid Ground State in a Random Quantum Heisenberg Magnet, Phys. Rev. Lett. **70**, 3339 (1993).

[2] A. Y. Kitaev, KITP Program: *Entanglement in Strongly-Correlated Quantum Matter* (University of California, Santa Barbara, 2015), available at https://online.kitp.ucsb.edu/online/entangled15/.

[3] S. Sachdev, Bekenstein-Hawking Entropy and Strange Metals, Phys. Rev. X **5**, 041025 (2015).

[4] O. Parcollet and A. Georges, Non-Fermi-liquid regime of a doped Mott insulator, Phys. Rev. B **59**, 5341 (1999).

[5] J. Polchinski and V. Rosenhaus, The spectrum in the Sachdev-Ye-Kitaev model, J. High Energy Phys. 04 (2016) 1.

[6] J. Maldacena and D. Stanford, Remarks on the Sachdev-Ye-Kitaev model, Phys. Rev. D **94**, 106002 (2016).

[7] A. Kitaev and S. J. Suh, The soft mode in the Sachdev-Ye-Kitaev model and its gravity dual, J. High Energy Phys. 05 (2018) 183.

[8] D. J. Gross and V. Rosenhaus, All point correlation functions in SYK, J. High Energy Phys. 12 (2017) 148.

[9] A. Georges, O. Parcollet, and S. Sachdev, Quantum fluctuations of a nearly critical Heisenberg spin glass, Phys. Rev. B **63**, 134406 (2001).

[10] R. A. Davison, W. Fu, A. Georges, Y. Gu, K. Jensen, and S. Sachdev, Thermoelectric transport in disordered metals without quasiparticles: The Sachdev-Ye-Kitaev models and holography, Phys. Rev. B **95**, 155131 (2017).

[11] Y. Gu, A. Kitaev, S. Sachdev, and G. Tarnopolsky, Notes on the complex Sachdev-Ye-Kitaev model, J. High Energy Phys. 02 (2020) 157.

[12] B. Keimer, R. J. Birgeneau, A. Cassanho, Y. Endoh, R. W. Erwin, M. A. Kastner, and G. Shirane, Scaling Behavior of the Generalized Susceptibility in $La_{2-x}Sr_xCuO_{4+y}$, Phys. Rev. Lett. **67**, 1930 (1991).

[13] M. C. Aronson, R. Osborn, R. A. Robinson, J. W. Lynn, R. Chau, C. L. Seaman, and M. B. Maple, Non-Fermi-Liquid Scaling of the Magnetic Response in $UCu_{5-x}Pd_x$ ($x = 1, 1.5$), Phys. Rev. Lett. **75**, 725 (1995).

[14] G. Aeppli, T. E. Mason, S. M. Hayden, H. A. Mook, and J. Kulda, Nearly singular magnetic fluctuations in the normal state of a high-T_c cuprate superconductor, Science **278**, 1432 (1997).

[15] A. Schröder, G. Aeppli, E. Bucher, R. Ramazashvili, and P. Coleman, Scaling of Magnetic Fluctuations near a Quantum Phase Transition, Phys. Rev. Lett. **80**, 5623 (1998).

[16] W. J. Gannon, L. S. Wu, I. A. Zaliznyak, W. H. Xu, A. M. Tsvelik, Y. Qiu, J. A. Rodriguez-Rivera, and M. C. Aronson, Local quantum phase transition in YFe_2Al_{10}, Proc. Natl. Acad. Sci. U.S.A. **115**, 6995 (2018).

[17] D. G. Joshi and S. Sachdev, Anomalous density fluctuations in a random t-J model, Phys. Rev. B **102**, 165146 (2020).

[18] M. Mitrano, A. A. Husain, S. Vig, A. Kogar, M. S. Rak, S. I. Rubeck, J. Schmalian, B. Uchoa, J. Schneeloch, R. Zhong, G. D. Gu, and P. Abbamonte, Anomalous density fluctuations in a strange metal, Proc. Natl. Acad. Sci. U.S.A. **115**, 5392 (2018).

[19] A. A. Husain, M. Mitrano, M. S. Rak, S. Rubeck, B. Uchoa, K. March, C. Dwyer, J. Schneeloch, R. Zhong, G. D. Gu, and P. Abbamonte, Crossover of Charge Fluctuations across the Strange Metal Phase Diagram, Phys. Rev. X **9**, 041062 (2019).

[20] M. Tikhanovskaya, H. Guo, S. Sachdev, and G. Tarnopolsky, following paper, Excitation spectra of quantum matter without quasiparticles. II. Random t-J models, Phys. Rev. B **103**, 075142 (2021).

[21] D. G. Joshi, C. Li, G. Tarnopolsky, A. Georges, and S. Sachdev, Deconfined Critical Point in a Doped Random Quantum Heisenberg Magnet, Phys. Rev. X **10**, 021033 (2020).

[22] H. Guo, Y. Gu, and S. Sachdev, Linear in temperature resistivity in the limit of zero temperature from the time reparameterization soft mode, Ann. Phys. (NY) **418**, 168202 (2020).

[23] D. J. Gross and V. Rosenhaus, A Generalization of Sachdev-Ye-Kitaev, J. High Energy Phys. 02 (2017) 093.

[24] I. R. Klebanov and G. Tarnopolsky, Uncolored random tensors, melon diagrams, and the Sachdev-Ye-Kitaev models, Phys. Rev. D **95**, 046004 (2017).

[25] I. R. Klebanov, F. Popov, and G. Tarnopolsky, TASI lectures on large N tensor models, Proc. Sci. **305**, 004 (2018).

[26] D. J. Gross and V. Rosenhaus, The Bulk Dual of SYK: Cubic Couplings, J. High Energy Phys. 05 (2017) 092.

[27] D. J. Gross and V. Rosenhaus, A line of CFTs: From generalized free fields to SYK, J. High Energy Phys. 07 (2017) 086.

[28] J. S. Cotler, G. Gur-Ari, M. Hanada, J. Polchinski, P. Saad, S. H. Shenker, D. Stanford, A. Streicher, and M. Tezuka, Black holes and random matrices, J. High Energy Phys. 05 (2017) 118; 09 (2018) 002.

[29] D. B. Kaplan, J.-W. Lee, D. T. Son, and M. A. Stephanov, Conformality lost, Phys. Rev. D **80**, 125005 (2009).

[30] S. Giombi, I. R. Klebanov, and G. Tarnopolsky, Conformal QED$_d$, F-theorem and the ϵ expansion, J. Phys. A: Math. Theor. **49**, 135403 (2016).

[31] V. Gorbenko, S. Rychkov, and B. Zan, Walking, Weak first-order transitions, and complex CFTs, J. High Energy Phys. 10 (2018) 108.

[32] S. Giombi, I. R. Klebanov, F. Popov, S. Prakash, and G. Tarnopolsky, Prismatic large N models for bosonic tensors, Phys. Rev. D **98**, 105005 (2018).

[33] J. Kim, I. R. Klebanov, G. Tarnopolsky, and W. Zhao, Symmetry Breaking in Coupled SYK or Tensor Models, Phys. Rev. X **9**, 021043 (2019).

[34] R. Nobili, Conformal covariant Wightman functions, Nuovo Cimento A **13**, 129 (1973).

[35] L. Iliesiu, F. Kos, D. Poland, S. S. Pufu, D. Simmons-Duffin, and R. Yacoby, Bootstrapping 3D fermions, J. High Energy Phys. 03 (2016) 120.

[36] A. Kitaev, Notes on $\widetilde{SL}(2, \mathbb{R})$ representations, arXiv:1711.08169.

[37] L. F. Cugliandolo, D. R. Grempel, and C. A. da Silva Santos, From Second to First Order Transitions in a Disordered Quantum Magnet, Phys. Rev. Lett. **85**, 2589 (2000).

[38] L. F. Cugliandolo, D. R. Grempel, and C. A. da Silva Santos, Imaginary-time replica formalism study of a quantum spherical p-spin-glass model, Phys. Rev. B **64**, 014403 (2001).

[39] J. Murugan, D. Stanford, and E. Witten, More on supersymmetric and 2d analogs of the SYK model, J. High Energy Phys. 08 (2017) 146.

[40] S. Giombi, I. R. Klebanov, and G. Tarnopolsky, Bosonic tensor models at large N and small ϵ, Phys. Rev. D **96**, 106014 (2017).

[41] E. Tulipman and E. Berg, Strongly coupled quantum phonon fluid in a solvable model, Phys. Rev. Res. **2**, 033431 (2020).

[42] W. Fu, Y. Gu, S. Sachdev, and G. Tarnopolsky, $\mathbb{Z}_2$ fractionalized phases of a solvable, disordered, t-J model, Phys. Rev. B **98**, 075150 (2018).

[43] D. Mao, D. Chowdhury, and T. Senthil, Slow scrambling and hidden integrability in a random rotor model, Phys. Rev. B **102**, 094306 (2020).

[44] A. Abanov and A. V. Chubukov, Interplay between superconductivity and non-Fermi liquid at a quantum critical point in a metal. I." Phys. Rev. B **102**, 024524 (2020).

[45] T. Azeyanagi, F. Ferrari, and F. I. Schaposnik Massolo, Phase Diagram of Planar Matrix Quantum Mechanics, Tensor, and Sachdev-Ye-Kitaev Models, Phys. Rev. Lett. **120**, 061602 (2018).

[46] F. Ferrari and F. I. Schaposnik Massolo, Phases of melonic quantum mechanics, Phys. Rev. D **100**, 026007 (2019).

[47] Y. Gu and P. Zhang " (unpublished)".

[48] D. Bagrets, A. Altland, and A. Kamenev, Sachdev–Ye–Kitaev model as Liouville quantum mechanics, Nucl. Phys. B **911**, 191 (2016).

[49] T. G. Mertens, G. J. Turiaci, and H. L. Verlinde, Solving the Schwarzian via the conformal bootstrap, J. High Energy Phys. 08 (2017) 136.

[50] B. Kobrin, Z. Yang, G. D. Kahanamoku-Meyer, C. T. Olund, J. E. Moore, D. Stanford, and N. Y. Yao, Many-Body Chaos in the Sachdev-Ye-Kitaev Model, Phys. Rev. Lett. **126**, 030602 (2021).

[51] A. Kruchkov, A. A. Patel, P. Kim, and S. Sachdev, Thermoelectric power of Sachdev-Ye-Kitaev islands: Probing Bekenstein-Hawking entropy in quantum matter experiments, Phys. Rev. B **101**, 205148 (2020).

[52] M. Vojta, C. Buragohain, and S. Sachdev, Quantum impurity dynamics in two-dimensional antiferromagnets and superconductors, Phys. Rev. B **61**, 15152 (2000).

[53] S. Sachdev, Static hole in a critical antiferromagnet: Field-theoretic renormalization group, Physica C **357**, 78 (2001).

[54] I. R. Klebanov, S. S. Pufu, and B. R. Safdi, F-theorem without supersymmetry, J. High Energy Phys. 10 (2011) 038.

[55] L. Fei, S. Giombi, I. R. Klebanov, and G. Tarnopolsky, Generalized F-theorem and the ϵ expansion, J. High Energy Phys. 12 (2015) 1.

[56] J. Maldacena, D. Stanford, and Z. Yang, Conformal symmetry and its breaking in two dimensional nearly anti–de Sitter space, Prog. Theor. Exp. Phys. **2016**, 12C104 (2016).

[57] E. Katz, S. Sachdev, E. S. Sørensen, and W. Witczak-Krempa, Conformal field theories at nonzero temperature: Operator product expansions, Monte Carlo, and holography, Phys. Rev. B **90**, 245109 (2014).

[58] L. Iliesiu, M. Koloğlu, R. Mahajan, E. Perlmutter, and D. Simmons-Duffin, The conformal bootstrap at finite temperature, J. High Energy Phys. 10 (2018) 070.

[59] G. Tarnopolsky, Large q expansion in the Sachdev-Ye-Kitaev model, Phys. Rev. D **99**, 026010 (2019).